
Effect of AAR on Shear Strength of Panels

TASK 1-C

DECEMBER 2017

BY

VICTOR E. SAOUMA

DAVID GRAFF

DAMON HOWARD

MOHAMMAD AMIN HARIRI-ARDEBILI

University of Colorado, Boulder

NRC-HQ-60-14-G-0010: REPORTS

1-A: *Design of an AAR Prone Concrete Mix for Large Scale Testing*

1-B: *AAR Expansion; Effect of Reinforcement, Specimen Type, and Temperature*

1-C: *Effect of AAR on Shear Strength of Panels*

2: *Diagnosis & Prognosis of AAR in Existing Structures*

3-A: *Risk Based Assessment of the Effect of AAR on Shear Walls Strength*

3-B: *Probabilistic Based Nonlinear Seismic Analysis of Nuclear Containment Vessel Structures with AAR*

Contents

| | | |
|-----------|---|-----------|
| I | Introduction | 11 |
| 1 | Introduction | 13 |
| 1.1 | Motivation | 13 |
| 1.2 | Test Setup | 14 |
| 1.3 | End Plates | 17 |
| 1.4 | Reinforcement | 17 |
| 1.5 | From Container to Specimen | 20 |
| 1.6 | Load Determination | 21 |
| 1.6.1 | Based on Scaling | 21 |
| 1.6.2 | Testing Equipment Considerations | 22 |
| 1.6.3 | Selected Traction | 23 |
| 2 | Specimen Design, Casting and Curing | 25 |
| 2.1 | Formwork | 25 |
| 2.2 | Casting | 26 |
| 2.3 | Concrete Compressive Strength Testing | 29 |
| 2.4 | Curing | 30 |
| 2.5 | Expansion Measurements | 33 |
| II | Testing Protocol | 35 |
| 3 | Pre-Mortem | 37 |
| 3.1 | From Fog Room to Testing Machine | 37 |
| 3.1.1 | Specimen Removal | 37 |
| 3.1.2 | Notch | 37 |
| 3.1.3 | Splitting Tensile Strength | 37 |
| 3.1.4 | Mark the Specimen | 37 |
| 3.2 | Installation Procedure | 38 |
| 3.2.1 | Nomenclature | 38 |
| 3.2.2 | Cheklis t | 39 |
| 3.3 | Pre-Tests Pictures | 42 |

| | |
|--|-----------|
| 3.4 Concrete Properties | 50 |
| 3.4.1 Compressive Strength | 50 |
| 3.4.2 Splitting Tensile Strength | 50 |
| 3.4.3 Measured f_c f_t relationships | 50 |
| 4 Testing | 53 |
| 4.1 Test Peparation | 53 |
| 4.1.1 Equipment preparation | 53 |
| 4.1.2 Wiring connections | 53 |
| 4.1.3 Position switches, start software | 55 |
| 4.1.4 Configure the settings | 56 |
| 4.1.5 Prepare for the test | 56 |
| 4.2 Testing | 56 |
| 4.2.1 LabView Operation | 56 |
| 4.2.2 Notification | 57 |
| 4.2.3 Crack Identification | 57 |
| 4.3 Test Termination | 57 |
| 4.3.1 Safe the Specimen | 57 |
| 4.3.2 Save data, shut down | 57 |
| 4.3.3 Unhook wires | 58 |
| 5 Post-Mortem | 59 |
| 5.1 Test Notes | 59 |
| 5.2 Cracks and Pictures | 61 |
| III Test Results | 65 |
| 6 Test Results | 66 |
| 6.1 Test Matrix | 66 |
| 6.2 Analysis Strategy | 67 |
| 6.3 Expansion Measurements | 67 |
| 6.4 Test Results | 68 |
| 6.5 Finite Element Simulation | 69 |
| 6.6 Analysis of Results | 71 |
| 7 Observations and Conclusions | 75 |
| References | 77 |
| Index | 78 |
| Appendices | 81 |
| A Test Data Acquisition and Control | 81 |
| A.1 Instrumentation | 82 |

| | |
|---------------------------------|-----------|
| A.2 Control | 84 |
| A.3 Hydraulics | 85 |
| B Calibration | 87 |
| B.1 MTS Calibration | 87 |
| C Assembly of Test Setup | 89 |

List of Figures

| | | |
|------|---|----|
| 1.1 | Prototype NCVS adopted for this study (NUREG/CR-6706, 2001) | 14 |
| 1.2 | Free Body Diagram of the experimental setup | 15 |
| 1.3 | Specimen details | 15 |
| 1.4 | Specimen dimensions | 16 |
| 1.5 | Experimental Setup | 16 |
| 1.6 | NCV Model and Prototype | 16 |
| 1.7 | End plates with shear studs | 17 |
| 1.8 | Explanation of reinforcement selection | 18 |
| 1.9 | Reinforcement arrangement | 20 |
| 1.10 | Interaction between model and specimens | 21 |
| 1.11 | Actuator forces in terms of the depth of concrete h | 23 |
| 2.1 | Shear specimen form preparation | 25 |
| 2.2 | Shipment of specimens to casting location | 26 |
| 2.3 | Wood forms built, transported, and organized at casting location | 26 |
| 2.4 | Mixing aggregates for consistent moisture content | 27 |
| 2.5 | Loading aggregates into batcher | 27 |
| 2.6 | Adding water, aggregates, and cement to mixer | 28 |
| 2.7 | Pouring mixed cement from mixer for testing and transportation to forms | 28 |
| 2.8 | Slump and air content testing | 28 |
| 2.9 | Filling forms, vibrating concrete, and covering with wetted burlap | 28 |
| 2.10 | Compression Testing | 29 |
| 2.11 | Specimen | 30 |
| 2.12 | Electric space used to heat the fog room during heat installation | 30 |
| 2.13 | Installation of reactive and non-reactive specimens in the fog room and computer for data logging | 31 |
| 2.14 | Placing shear specimen in fog room with forklift | 31 |
| 2.15 | Sprinkler system for the specimens | 32 |
| 2.16 | Sump pumps used to power sprinkler system | 32 |
| 2.17 | Expansion measurements | 33 |
| 3.1 | Specimen description | 38 |
| 3.2 | Specimen and cage about to be installed | 40 |

| | | |
|------|--|----|
| 3.3 | S1 | 42 |
| 3.4 | S2 | 43 |
| 3.5 | S3 | 43 |
| 3.6 | S4 | 44 |
| 3.7 | S5 | 44 |
| 3.8 | S6 | 45 |
| 3.9 | S7 | 45 |
| 3.10 | S8 | 46 |
| 3.11 | S9 | 46 |
| 3.12 | S10 | 47 |
| 3.13 | S11 | 47 |
| 3.14 | S12 | 48 |
| 3.15 | S13 | 48 |
| 3.16 | S14 | 48 |
| 3.17 | S15 | 49 |
| 3.18 | S16 | 49 |
| 3.19 | Compressive <i>vs</i> tensile splitting strengths | 52 |
| 4.1 | Connections from SCXI-1314 terminal block | 53 |
| 4.2 | Valve front pressure connection | 54 |
| 4.3 | Force Displacement connections | 54 |
| 4.4 | Setup details | 55 |
| 5.1 | <i>Post-Mortem</i> pictures of specimens 1 to 9 | 62 |
| 5.2 | <i>Post-Mortem</i> pictures of specimens 10 to 16 | 63 |
| 6.1 | Test Matrix | 67 |
| 6.2 | AAR expansion in tested concrete specimens | 68 |
| 6.3 | FEA computed load displacement curves. | 70 |
| 6.4 | Computed internal cracking in terms of load displacement curve | 71 |
| 6.5 | Experimental and numerical results | 71 |
| 6.6 | Normalized experimental and numerical results | 72 |
| A.1 | MTS million-pound load frame | 81 |
| A.2 | Eaton hydraulic actuators | 82 |
| A.3 | National Instruments PXI-1042Q with embedded controller, data acquisition, and command | 82 |
| A.4 | Omega pressure transducer | 83 |
| A.5 | LVDT body | 84 |
| A.6 | Pressure-control flow diagram | 84 |
| A.7 | Crack opening flow diagram | 85 |
| A.8 | Hydraulic oil distribution and command | 86 |
| B.1 | Calibration of the Million lbf MTS | 87 |

| | |
|--|----|
| C.1 Setup Installation as of Jan 15. Specimen “cage” (lower right) will be assembled and proof tested next | 89 |
| C.2 Assembly of test setup | 90 |

List of Tables

| | | |
|-----|--|----|
| 1.1 | Prototype and model containment vessel dimensions | 15 |
| 1.2 | Hoop reinforcement (Blue) ratio selection | 19 |
| 1.3 | Longitudinal reinforcement (Red) ratio selection | 19 |
| 1.4 | Panel reinforcement (all dimensions in inches) | 19 |
| 2.1 | Shear specimens cast | 27 |
| 2.2 | Slump of each concrete batch | 29 |
| 2.3 | Average 7 and 28 Day Compressive Strength | 29 |
| 3.1 | Measured compressive strengths at 7 and 28 days | 50 |
| 3.2 | Splitting Tensile Strengths (psi) | 51 |
| 6.1 | Shear specimens cast | 66 |
| 6.2 | Experimental results | 69 |
| 6.3 | Details and results of FEA along with experimental results | 70 |
| 6.4 | Statistical analysis of results | 73 |

Acknowledgments

The shear setup was engineered, designed and built by Prof. Volker Slowik (Leipzig University of Applied Sciences) during a visit at the University of Colorado in support for EPRI and TEPCO projects. His continuous support and advices are gratefully acknowledged.

This page intentionally left blank.

Part I

Introduction

This page intentionally left blank.

1— Introduction

1.1 Motivation

Motivation Though AAR has been known to affect numerous structures, dams in particular (ICOLD Bulletin 79, 1991) (Amberg, 2011), only recently has it been found in one or more nuclear containment structures (Saouma, 2013). Despite the lack of publicity, some nuclear power plants reactors are starting to show signs of ASR, (*ibid.*). In Japan, the (reinforced concrete) turbine generator foundation at Ikata No. 1 NPP (owned by Shihoku Electric Power) exhibits ASR expansion and has thus been the subject of many studies. Takatura et al. (2005a) reports on the field investigation work underway: location, extent of cracking, variation in concrete elastic modulus and compressive strength, expansion in sufficient detail to adequately understand the extent of damage. The influence of ASR on mechanical properties (in particular, the influence of rebar) and on structural behavior has been discussed by Murazumi et al. (2005a) and Murazumi et al. (2005b), respectively. In the latter study, beams made from reactive concrete were tested for shear and flexure. These beams were cured at 40°C and 100% relative humidity for about six weeks. Some doubt remains, however, as to how representative such a beam is for those NPP where ASR has been occurring for over 30 years. A study of the material properties introduced in the structural analysis was first reported by Shimizu et al. (2005b). An investigation of the safety margin for the turbine generator foundation has also been conducted (Shimizu et al., 2005a). Moreover, vibration measurements and simulation analyses have been performed (Takatura et al., 2005b). Takagura et al. (2005) has recently reported on an update of the safety assessment at this NPP. In Canada, Gentilly 2 NPP is known to have suffered ASR (Orbovic, 2011). An early study by Tcherner and Aziz (2009) actually assessed the effects of ASR on a CANDUTM6 NPP (such as Gentilly 2). In 2012 however, following an early attempt to extend the life of Gentilly 2 until 2040 (with an approx. \$1.9B overhaul), Hydro-Quebec announced its decommissioning after 29 years for economic reasons. Yet, as late as 2007, it was reported that *to date, no incidences of ASR-related damage have been identified in U.S. nuclear power plants* (Naus, 2007).

US designed nuclear containment vessels (NCV) do not have shear reinforcement by design. Yet, should they be affected by alkali aggregate reaction (AAR) there would be great concern as to their ability to withstand the horizontal forces induced by a seismic excitation. As such, recent research programs have addressed the shear strength of AAR affected shear walls (Orbovic et al., 2015) or beams (ADAMS Accession No. ML 121160422, 2012).

This report details an experimental program undertaken at the university of Colorado to assess the impact of AAR on the seismic resistance of a NCV.

1.2 Test Setup

This research will subject a concrete panel, representative of a segment of the NCV to lateral compressive confinement in one direction, and will shear it in the orthogonal one, Fig. 1.2.

For reference dimension, the representative NCVS shown in Fig. 1.1 , (NUREG/CR-6706, 2001). It should be noted that the same geometry is adopted for the nonlinear transient finite element study of a NCVS with both AAR and subjected to seismic excitation (Saouma, 2017).

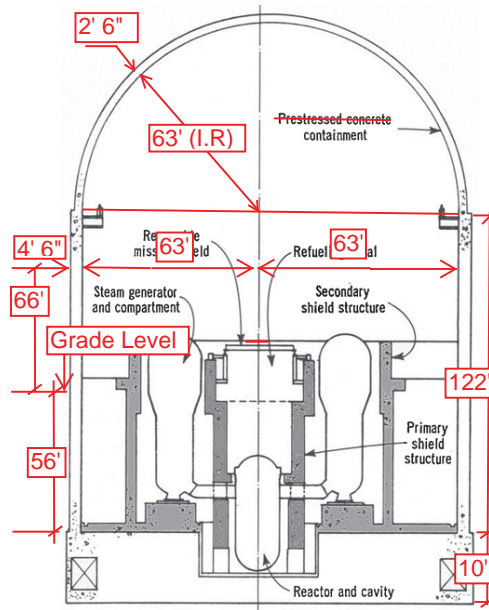


Figure 1.1: Prototype NCVS adopted for this study (NUREG/CR-6706, 2001)

Whereas preliminary design had the shear load entirely applied from the side, following preliminary tests the specimen cage was not deemed to be stiff enough for such a transfer, Hence, the shear force (blue) is applied both vertically and laterally. Lateral confinement (green) is to prevent rotation and to simulate the actual normal traction anticipated. The anticipated crack is shown in dashed line, it corresponds to a compressive strut caused by the load transfer mechanism. This conceptual model translates into a specimen configuration shown in Fig. 1.3, with actual dimensions shown in Fig. 1.4. The specimen is then loaded into the million pound test frame, Fig. 1.5.

Since, the testing machine can only accommodate a finite specimen size, the controlling factor is the height of the specimen which should ideally correspond to the thickness of the NCV (4.5 ft). The specimen height being 30 in. (or 2.5 ft), a scale factor $\lambda = 2.5/4.5 = 0.56$ is adopted for the test. Table 1.1 shows the dimensions for a representative NCV prototype and its model. The relationship between the two is further illustrated by Fig. 1.6.

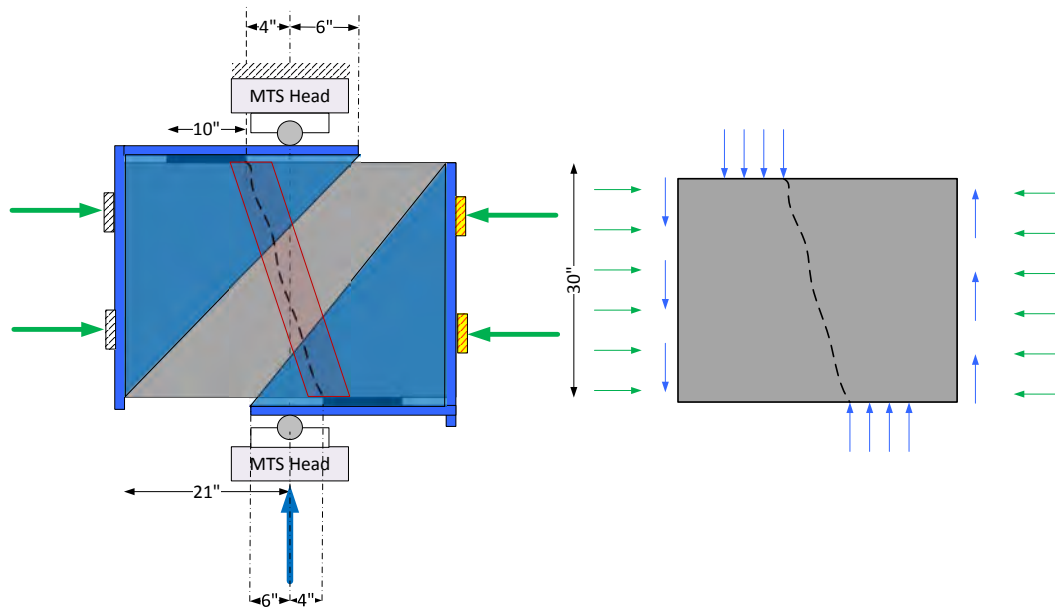


Figure 1.2: Free Body Diagram of the experimental setup

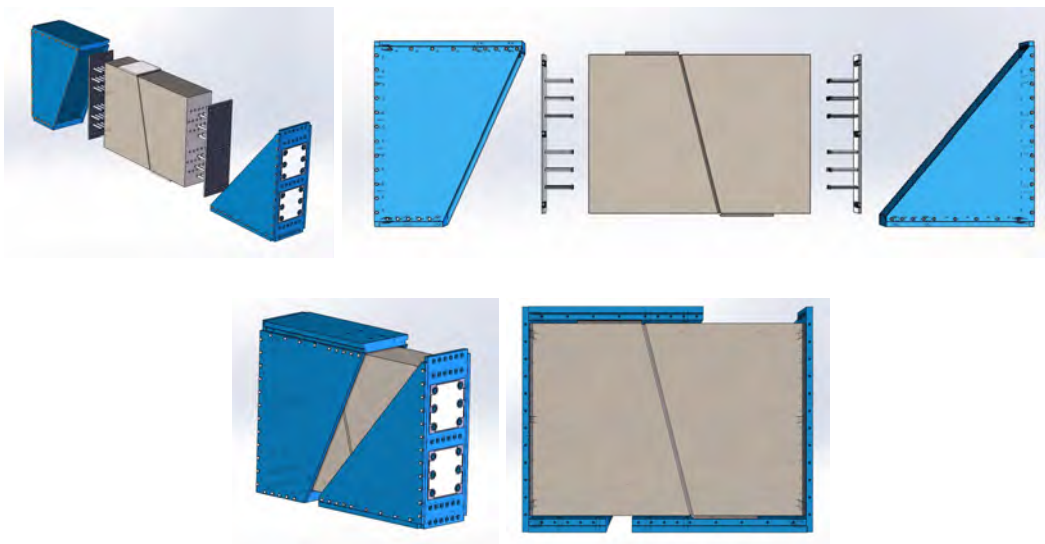


Figure 1.3: Specimen details

Table 1.1: Prototype and model containment vessel dimensions

| Parameter | Prototype | Model |
|-------------------------------------|-----------|-------|
| Scale factor | 1.00 | 0.56 |
| Inner radius (ft) | 63.0 | 35.0 |
| Wall thickness (ft) | 4.5 | 2.5 |
| Wall height (ft) | 122.0 | 68.0 |
| Foundation thickness (ft) | 10.0 | 5.6 |
| Grade level - above foundation (ft) | 56.0 | 31.3 |
| Dome thickness (ft) | 2.6 | 1.5 |

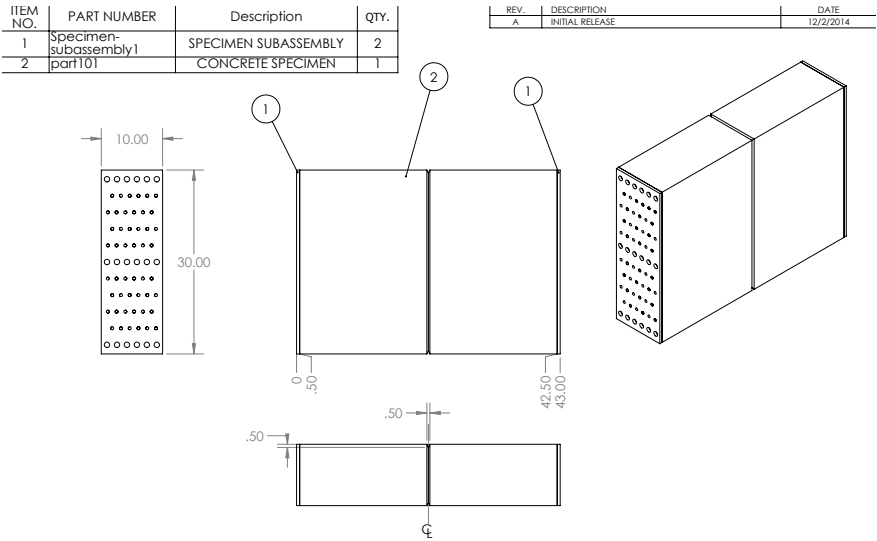


Figure 1.4: Specimen dimensions

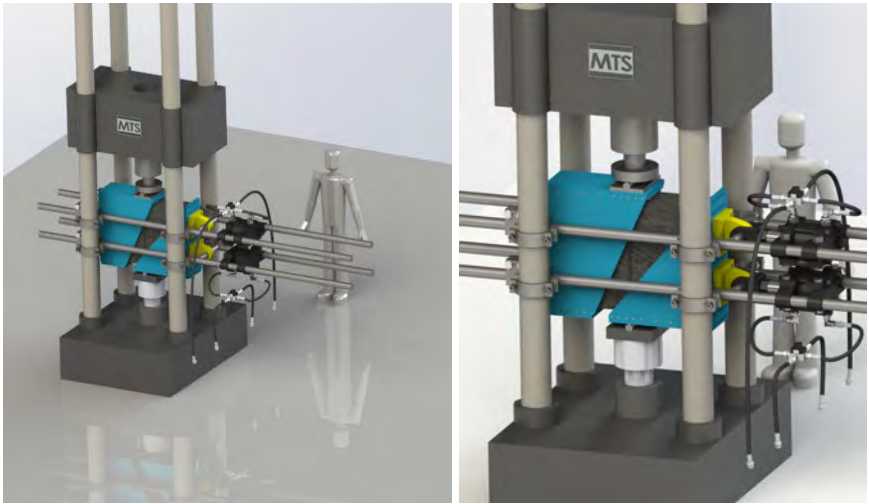


Figure 1.5: Experimental Setup

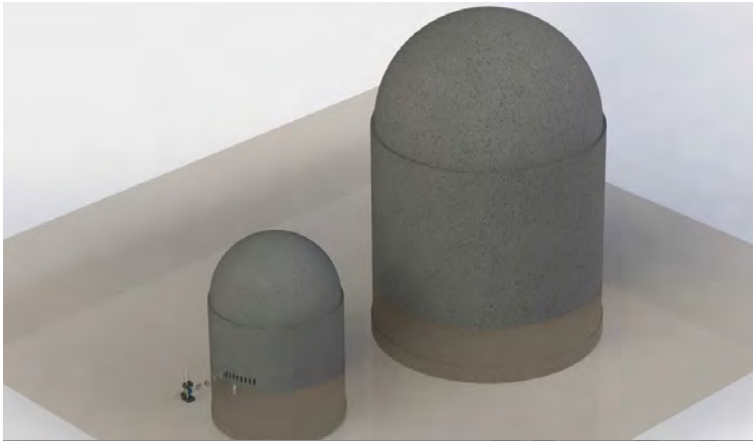
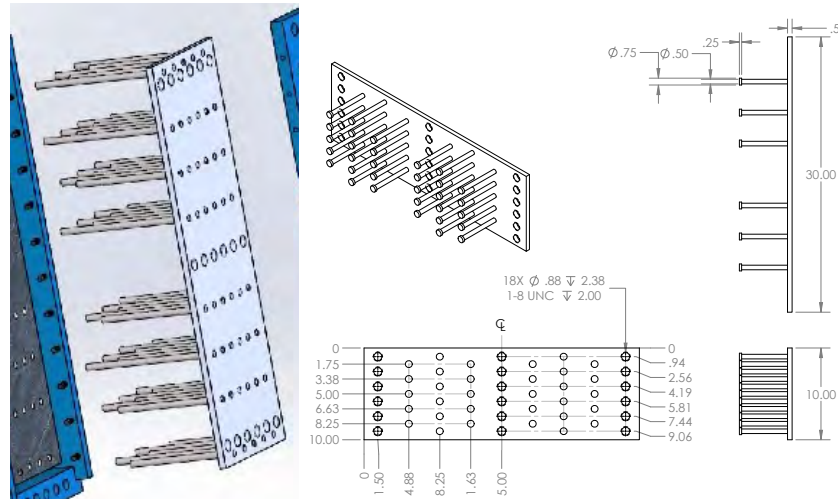


Figure 1.6: NCV Model and Prototype

1.3 End Plates

Steel plates are used at each end, and serve three purposes: a) provide “formwork” for the concrete; b) shear transfer to the concrete panel; and c) support for the reinforcement. Originally, the design called for 8 layers of long threaded rods, Fig. 1.7(a) as in past tests. However to accommodate the longitudinal reinforcement, and following proper calculations, it was found that 6 layers of shorter studs (with small end plate) should be enough, and thus the the design revised, Fig. 1.7(b) and 1.7(c).



(a) Original design of shear studs

(b) Internal specimen reinforcement



(c) Internal specimen reinforcement

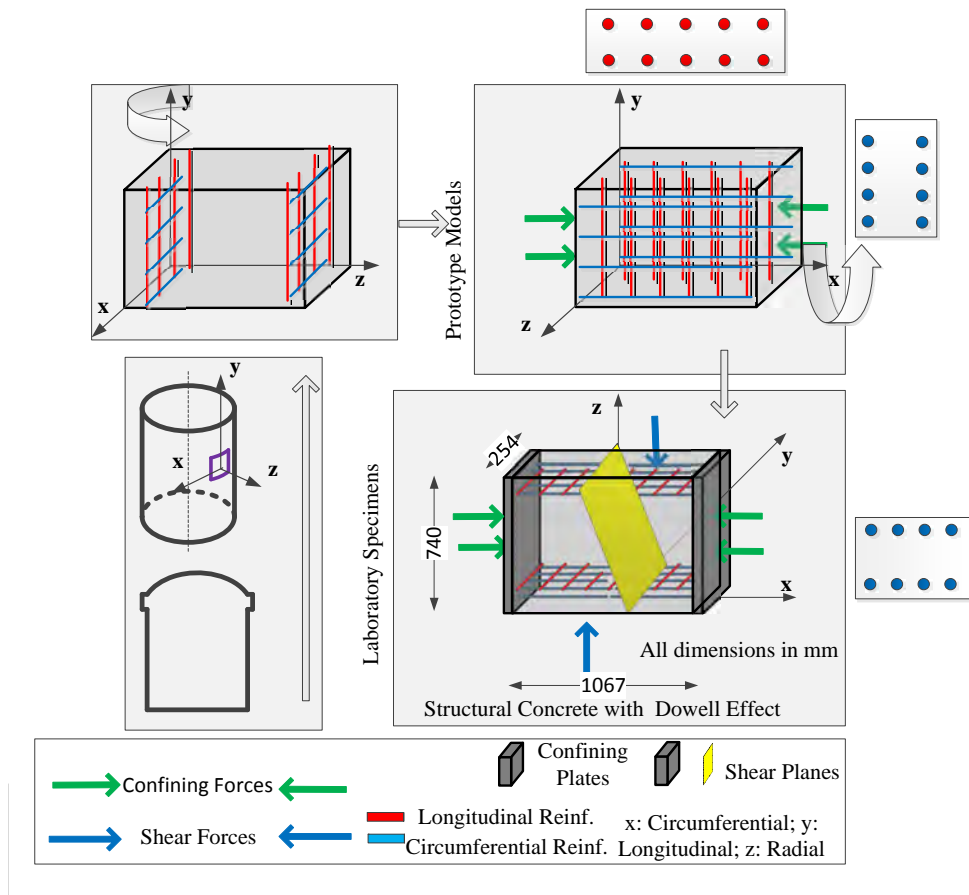
Figure 1.7: End plates with shear studs

1.4 Reinforcement

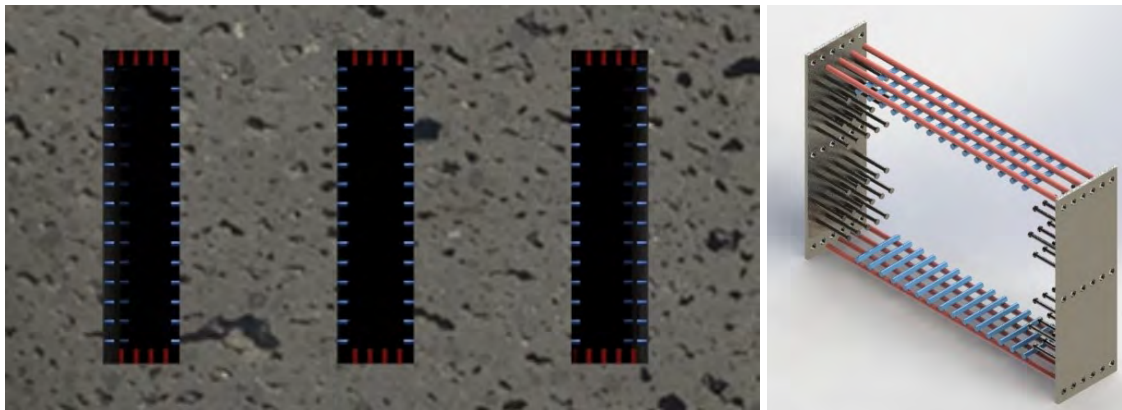
Some of the NCV in the US are prestressed, others have only mild steel reinforcement without any prestressing (as is the case of Seabrook). Furthermore, it is well known that internal reinforcement does provide expansion restraint. Hence, some of the specimens will have an internal reinforcement.

As shown in Fig. 1.8(a) the actual NCV will have hoop (blue) and longitudinal (red) reinforcement in the local x and y axes. Those are also shown in Fig. 1.8(b) from which the panel is extracted rotated with

respect to the y axis, and then with respect to the x axis to end up in the tested position, Fig. 1.8(c).



(a) Panel; From vessel to laboratory



(b) Reinforcement inside container

(c) Envisioned reinforcement

Figure 1.8: Explanation of reinforcement selection

Since reinforcement details of the prototype structure are not publicly available, reinforcement ratios were selected such that the resulting experimental specimens are both constructible and approximate typical NCV reinforcement. Various reinforcement ratios were considered and the number and size of bars required

to for each is presented in Table 1.2 and Table 1.3.

Table 1.2: Hoop reinforcement (Blue) ratio selection

| Dimensions | | H | 30 | Area (in ²) |
|--------------|-----------------------|----------------------|--------------------------------|-------------------------|
| | | W | 42 | 1,260 |
| Bar size (#) | X-Area A_{bar} (in) | Reinf. ratio, ρ | Required As (in ²) | # bars per layer |
| 5 | 0.31 | 0.20% | 2.52 | 9 |
| | | 0.50% | 6.3 | 21 |
| | | 1.00% | 12.6 | 41 |
| 6 | 0.44 | 0.20% | 2.52 | 6 |
| | | 0.50% | 6.3 | 15 |
| | | 1.00% | 12.6 | 29 |
| 7 | 0.6 | 0.20% | 2.52 | 5 |
| | | 0.50% | 6.3 | 11 |
| | | 1.00% | 12.6 | 21 |
| 8 | 0.79 | 0.20% | 2.52 | 4 |
| | | 0.50% | 6.3 | 8 |
| | | 1.00% | 12.6 | 16 |

Table 1.3: Longitudinal reinforcement (Red) ratio selection

| Dimensions | | H | 30 | Area (in ²) |
|--------------|-----------------------|----------------------|--------------------------------|-------------------------|
| | | W | 10 | 300 |
| Bar size (#) | X-Area A_{bar} (in) | Reinf. ratio, ρ | Required As (in ²) | # bars per layer |
| 4 | 0.2 | 0.20% | 0.6 | 3 |
| | | 0.50% | 1.5 | 8 |
| | | 1.00% | 3.0 | 15 |
| 5 | 0.31 | 0.20% | 0.6 | 2 |
| | | 0.50% | 1.5 | 5 |
| | | 1.00% | 3.0 | 10 |
| 6 | 0.44 | 0.20% | 0.6 | 2 |
| | | 0.50% | 1.5 | 4 |
| | | 1.00% | 3.0 | 7 |
| 7 | 0.6 | 0.20% | 0.6 | 1 |
| | | 0.50% | 1.5 | 3 |
| | | 1.00% | 3.0 | 5 |

Final reinforcement is provided by 4 #6 bars longitudinal (blue) and 11 #7 bars transversally (red), Table 1.4.

Table 1.4: Panel reinforcement (all dimensions in inches)

| | Bar | | | | # per layer | ρ | # bars per layer |
|--------------------|-----|----------|--------|---------|-------------|--------|------------------|
| | # | Diameter | Length | spacing | | | |
| Hoop (blue) | 7 | 0.875 | 8 | 2.81 | 11 | 0.52% | 11 |
| Longitudinal (red) | 6 | 0.75 | 42 | 2.08 | 4 | 0.59% | 4 |

With regard to anchorage, insufficient length was available for either the longitudinal or hoop steel to develop its full tensile strength. Considering the large strains anticipated due to ASR expansion, it is necessary to provide for some type of anchorage at the bar terminations. A number of options were

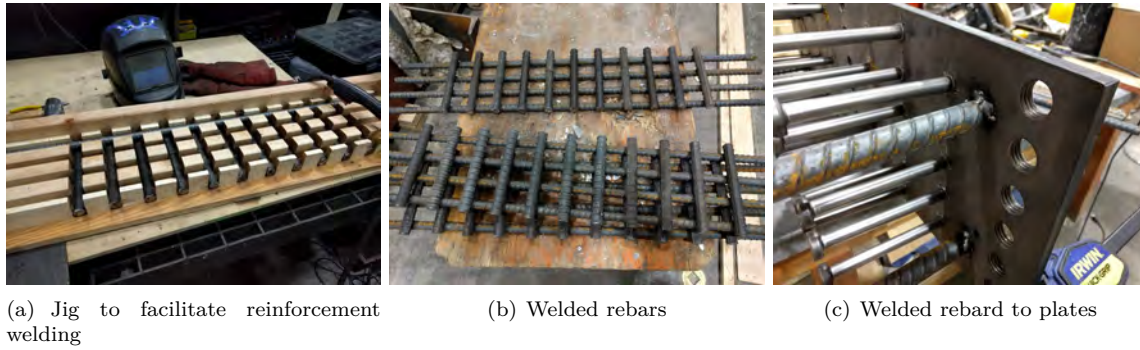


Figure 1.9: Reinforcement arrangement

considered, including hooks and threaded terminations. Unfortunately, the standard hook size for a #7 bar is 10.5" with a minimum bend diameter of 7". Considering that these bars are only 8" long, attempting to use standard hooks would deform the hoop reinforcement geometry to an extent that it would bear little resemblance to the prototype structure. Furthermore, the minimum development length even with hooks is 19" which exceeds the out-to-out thickness of the sample (10").

Ultimately, it was decided to weld axial bars to the sample end plates, and weld circumferential bars to the axial bars at each intersection. While welding rebar is not typically best practice, no other practical option existed for developing tensile strength in such a confined volume as the shear samples. The sample end plates did provide development for the longitudinal bars, while themselves act as hooks for the hoop bars. While certainly not ideal, this solution allowed for at least some tensile development without drastically altering the reinforcement scheme of the prototype system.

Given that a total of 330 bars had to be cut, the process was carefully planned and a wooden jig was assembled to facilitate welding, Fig. 1.9(a). The jig allowed rapid layout and welding of the rebar cages. The jig also provided a simple way to verify that all bars were cut to proper length. Any long or short bars would not fit properly into the jig and could be ground down or replaced.

Bars were MIG-welded to one another at each intersection. Care was taken to make small welds in order to minimize the size of heat-affected regions in the substrate bars, Fig. 1.9(b), and finally welded to the end plates, Fig. 1.9(c).

1.5 From Container to Specimen

Conceptually, the model can be seen as "extracted" from the NCV, rotated 90 degrees and then inserted in the load frame for testing, Fig. 1.10.

It is important to note that the circumferential reinforcement (in blue) correspond to the short transversal steel rods in the specimen, and that the vertical (red) ones to the axial reinforcement in the specimen.

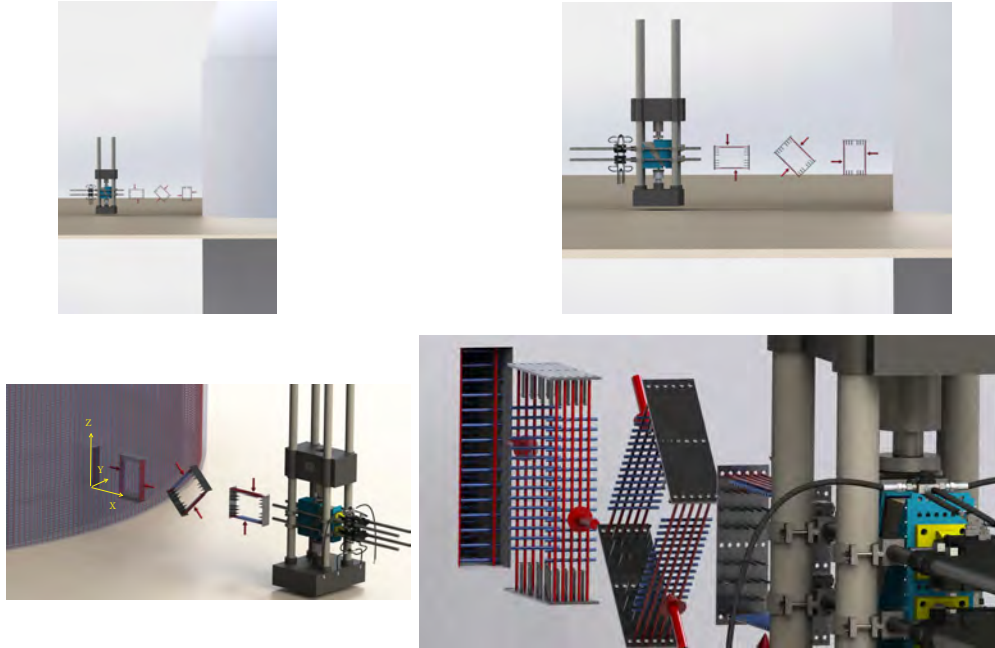


Figure 1.10: Interaction between model and specimens

1.6 Load Determination

1.6.1 Based on Scaling

Specimens should be subjected to shear forces corresponding to the most critical location (h measured from the base of the dome). At that location, the vertical force (due to weight of the concrete) should be determined, as it will be applied as a lateral force constraint by the two horizontal actuators in the experimental setup.

Another important consideration is the impact of a lateral seismic load on the normal base stress. Depending on the lateral excitation direction, the base of the NCVS will either experience a drastic increase or decrease in the normal stress. This effect is compounded by a vertical excitation.

Determination of the normal confining traction is important but not critical as all quantities will be later normalized.

There are two approaches to determine it. It should be noted, that all results will be normalized with respect to specimens with no AAR subjected to the same confinement.

Given:

| | | |
|-----------|------------------------|---|
| h | variable (ft) | point of critical shear force measured from the base of the dome. |
| R | 63 ft | Radius of NCVS |
| t_d | 2.6 ft | Dome thickness |
| t_c | 4.5 ft | Cylinder thickness |
| L_s | 30" | Model length (corresponding to thickness of prototype) |
| W_s | 10" | Width of model |
| λ | 0.56 | Scale factor |
| γ | 145 lb/ft ³ | Concrete weight density |

Cross-sectional area of the cylindrical part:

$$A_c = 2 \times \pi \times 63 \times 4.5 = 1,780[\text{ft}^2] \quad (1.1)$$

Volume of the cylindrical part

$$V_c = Ah = 1,780 \times h[\text{ft}^3] \quad (1.2)$$

Volume of dome

$$V_d = \frac{1}{2} \frac{4}{3} \left[(63 + 2.6)^3 - 63^3 \right] = 67,500[\text{ft}^3] \quad (1.3)$$

Total weight

$$W = 0.145 \times (1,780h + 67,500) \text{ Kips} \quad (1.4)$$

Base stress

$$\sigma = \frac{W}{A_c} = \frac{0.145 \times (1,780h + 67,500)}{144 \times 1,780} [\text{ksi}] \quad (1.5)$$

There are two approached to determine the actuator forces:

Model 1 Do not scale any dimension;

$$A1 = L_s \times W_s = 30 \times 10 = 300[\text{in}^2] \quad (1.6)$$

The corresponding total force to be applied by the two lateral actuators will be

$$F = \sigma \times A1 = \frac{0.145 \times (1,780h + 67,500)}{144 \times 1,780} \times 300 = 1.697 \times 10^{-4}(1,780h + 67,500) \quad (1.7)$$

Model 2 Scale both direction

$$A2 = \frac{L_s}{\lambda} \times \frac{W_s}{\lambda} = \frac{30}{0.56} \times \frac{10}{0.56} = 956.6[\text{in}^2] \quad (1.8)$$

The corresponding total force to be applied by the two lateral actuators will be

$$F = \sigma \times A2 = \frac{0.145 \times (1,780h + 67,500)}{144 \times 1,780} \times 956.6 = 5.41 \times 10^{-4}(1,780h + 67,500) \quad (1.9)$$

Fig. 1.11 shows the required lateral actuator forces in terms of the total depth of concrete below the base of the dome for the two cases considered. The three horizontal lines will be explained below.

1.6.2 Testing Equipment Considerations

Ideally, the two sets of testing equipment (Million pounds MTS for vertical shear forces) and the two lateral actuators (for the confining forces) should be able not only to apply the required forces, but the applied loads should fall within the range of proper calibration.

Typically, if the loads to be applied are relatively low compared to the capacity, then one would expect the load cell to give unreliable results as the calibration curve in this zone is nonlinear.

A total vertical force below $\simeq 200$ kips to be applied by the 1,000 kips MTS machine would be undesirable. Based on preliminary calculation, this required a lateral confining force of at least 50 kips.

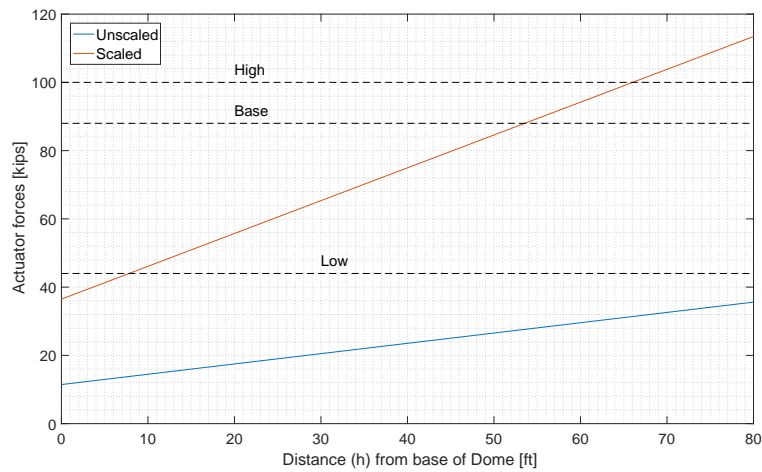


Figure 1.11: Actuator forces in terms of the depth of concrete h

1.6.3 Selected Traction

Based on the preceding considerations, it was determined that a nearly “optimal” set of confining forces should be, Fig.. 1.11:

Low: 44 kips.

Base: 88 kips.

High: 100 kips.

This page intentionally left blank.

2— Specimen Design, Casting and Curing

2.1 Formwork

Specimens will be cast horizontally, in order to better facilitate concrete penetration between closely-spaced shear studs. Thus a simple form was designed using 21/32" oriented-strand board and 2x4 studs. The top brace of the stud was elevated somewhat from the top surface of the concrete to allow a trowel to pass under during finishing. Corners are strengthened with steel brackets and the entire assembly is joined with deck screws. The form rests on its 2x4 braces, which allow it to be moved via forklift without extra blocking.

Two options for formwork material were considered. Either a small number of reusable forms could be constructed using more durable (but expensive) Plyform, or a larger number of single-use forms could be constructed using less-expensive oriented strand board (OSB). Since the large volume of concrete required necessitates that casting would be performed at the laboratory partner (Fall Line Testing and Inspection) in Denver, it was decided to adopt a compressed casting schedule to minimize impact on Fall Line business operations. Therefore, it was decided to construct single-use formwork.

Seventeen forms were built using OSB and 2"x4" studs, one for a dummy sample and sixteen for the experimental shear specimens. The upper brace visible in Fig. 2.1(a) is built to float above the surface of the concrete to allow a trowel finish to be applied. Formwork for additional block and prism specimens were produced in a similar fashion. To mitigate water absorption by the wood from the fresh concrete, the inside of each form was given two coats of oil-based primer, Fig. 2.1(b). Forms were assembled in Boulder, and then shipped to Fall Line Inspections LLC for casting, Fig. 2.2(a) where concrete was cast, Fig. 2.2(b).

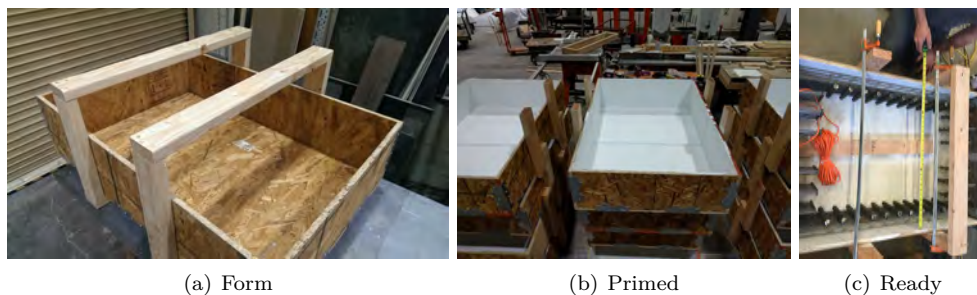


Figure 2.1: Shear specimen form preparation

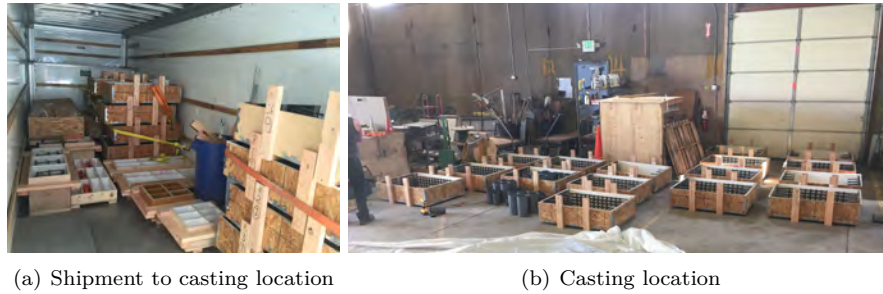


Figure 2.2: Shipment of specimens to casting location

2.2 Casting

The design concrete mix used was the subject of an 18 months investigation and is reported in Saouma, Sparks, and Graff (2016). This document includes the quantities of coarse and fine aggregate, water, cement, and admixtures for each batch. Additionally, mixed concrete properties such as slump, air content, unit weight, and water-cement ratio are detailed.

On May 2nd and 4th, 2016 the specimens to be used in this program were cast at Fall Line Inspections in Denver, CO. Over these two days, 6.27 cubic yards of concrete mixed and poured into forms to create 16 shear specimens, 15 blocks, 24 prisms, 9 wedge splitting test specimens, and multiple cylinders, Table 2.1. Figures 2.3 to 2.9 show a brief overview of the casting process including form building and transportation, aggregate preparation, concrete mixing, filling forms, and curing.

Finally, Table 2.1 lists the specimens which were cast. Shown are the concrete mixes associated with each specimen and whether an internal temperature gage is used and whether some of the reinforcement do have a strain gage.

Figure 2.3 shows the 16 shear specimen forms after being built, transporting them the Fall Line, and their organization in preparation for testing. Figure 2.4 shows mixing coarse and fine aggregates to provide constant moisture throughout the aggregates while batching and mixing. The aggregates are the loaded into the batcher in Figure 2.5. The batcher provides the correct weight of each aggregate in Figure 2.6 and transported to mixed via conveyor belt. Cement is weighed beforehand and manually added to the conveyor belt at the same time. Water is also weighed before mixing and added after the cement and aggregate. After cement is mixed, Figure 2.7 shows wet concrete poured out of mixer into bucket for easy transportation to the forms. Figure 2.8 shows slump and air content tests performed before filling forms ensuring adequate wet concrete properties are obtained. Finally, forms are filled, and concrete is vibrated in Figure 2.9. After forms are filled, concrete is covered with wet burlap to prevent shrinkage cracking.



Figure 2.3: Wood forms built, transported, and organized at casting location

Table 2.1: Shear specimens cast

| Mix | ID | Reactive | Rebars | Temp. ID | Strain Guage |
|-----|----|----------|--------|-------------|--------------|
| 1 | 1 | Y | Y | 1 | |
| | 2 | | Y | | |
| | 3 | | Y | | |
| 2 | 4 | Y | N | 2 | 9 |
| | 5 | | Y | | |
| | 6 | | Y | | |
| | 7 | | Y | | |
| | 8 | | N | | |
| 3 | 9 | Y | Y | 3 | 10 |
| | 10 | | Y | | |
| | 11 | | Y | | |
| | 12 | | N | | |
| 4 | 13 | No | Y | 4 | |
| | 14 | | Y | | |
| | 15 | | N | | |
| | 16 | | N | | |

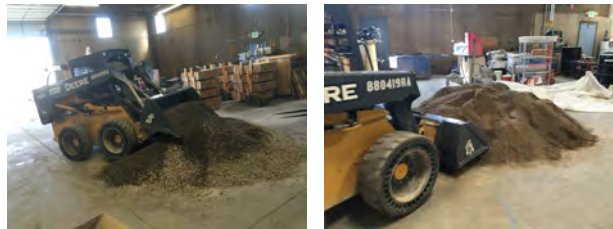


Figure 2.4: Mixing aggregates for consistent moisture content



Figure 2.5: Loading aggregates into batcher

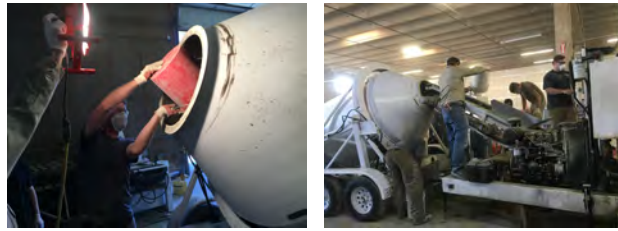


Figure 2.6: Adding water, aggregates, and cement to mixer

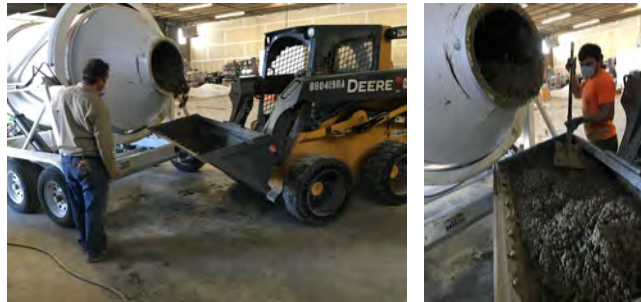


Figure 2.7: Pouring mixed cement from mixer for testing and transportation to forms



Figure 2.8: Slump and air content testing



Figure 2.9: Filling forms, vibrating concrete, and covering with wetted burlap

Table 2.2 gives the slump of each concrete batch cast. Batch 2 had a lower slump than the other batches and is outside the target range for the concrete mix. Due to time and material restraints, the concrete was still used and poured into forms.

| Batch Number | Slump (in) |
|--------------|------------|
| 1 | 5.5 |
| 2 | 2.25 |
| 3 | 6.0 |
| 4 | 4.75 |

Table 2.2: Slump of each concrete batch

2.3 Concrete Compressive Strength Testing

The concrete from each batch is tested to ensure that the concrete has reached the target 28-day compressive strength. 7 and 28 days after casting, three 4" cylinders from each concrete batch were tested in the 110-kip testing machine according to ASTM, C39 (2016), Figure 2.10. For each cylinder, three measurements were taken of they cylinder's diameter and length. Then it was placed in a machine under force controlled loading until failure. Figure shows a sample graph of the outputted data. Table 2.3 shows the average 7 and 28 day strength of each concrete batch. Note that all batches meet the target compressive strength of 4,000 psi.



Figure 2.10: Compression Testing

| Batch Number | Average 7-Day f'_c (ksi) | Average 28-Day f'_c (ksi) |
|--------------|----------------------------|-----------------------------|
| 1 | 2.64 | 5.99 |
| 2 | 4.13 | 4.98 |
| 3 | 3.67 | 4.21 |
| 4 | 4.83 | 5.71 |

Table 2.3: Average 7 and 28 Day Compressive Strength

2.4 Curing

Report ?? details the curing of the specimens, however for the sake of clarity some of the relevant details are repeated here.

CU Boulder's structures lab was used to store and cure a majority of the specimens. Using the room's integrated heaters and humidifiers, the room is kept as close to a constant temperature of 100°F and 95% relative humidity. Sensors are placed inside the room to monitor and log the temperature and humidity of the room.

Fig. 2.11 shows a cast specimen. All specimens were cast horizontally (in the y direction) to better facilitate concrete penetration between closely-spaced shear studs.

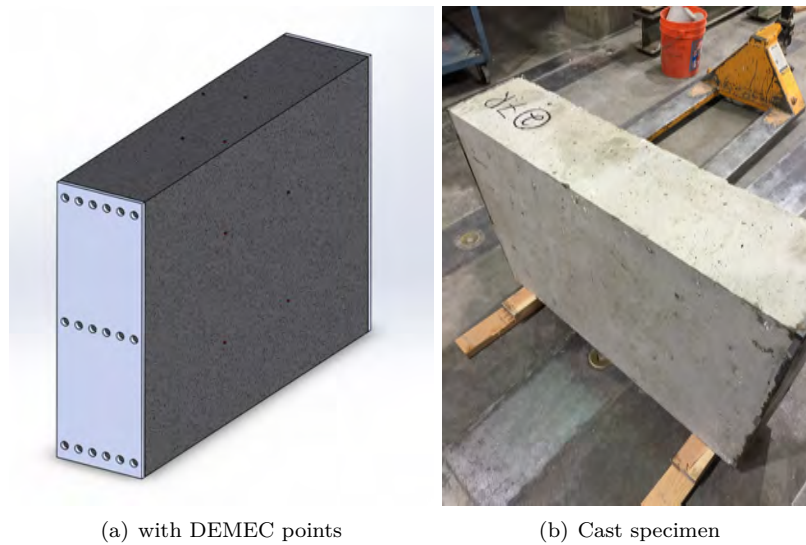


Figure 2.11: Specimen

In preparation for this research, it was discovered the existing fog room to not be properly operational. Facilities management has installed a new humidifier and upgraded the heat system by connecting to the steam that is available in the building that will provide heat year round. To provide heat during this installation, electric space heaters, shown in Figure 2.12, were installed in the fog room to keep the room as close to 100°F. Ultimately five space heaters had to be used to get to the target temperature.



Figure 2.12: Electric space used to heat the fog room during heat installation

The pans had to be thoughtfully oriented in the fog room in such a way that each shear specimen can be brought in using a forklift. The forklift will support a spreader bar that lifts two straps that are wrapped under the bottom of the sample, Fig. 2.13. A “first in, last out” plan was implemented when placing specimens in to the fog room to minimize the amount of moving samples around during the removal process. However, this will be somewhat controlled by the expansion levels of each specimen at the time of testing.

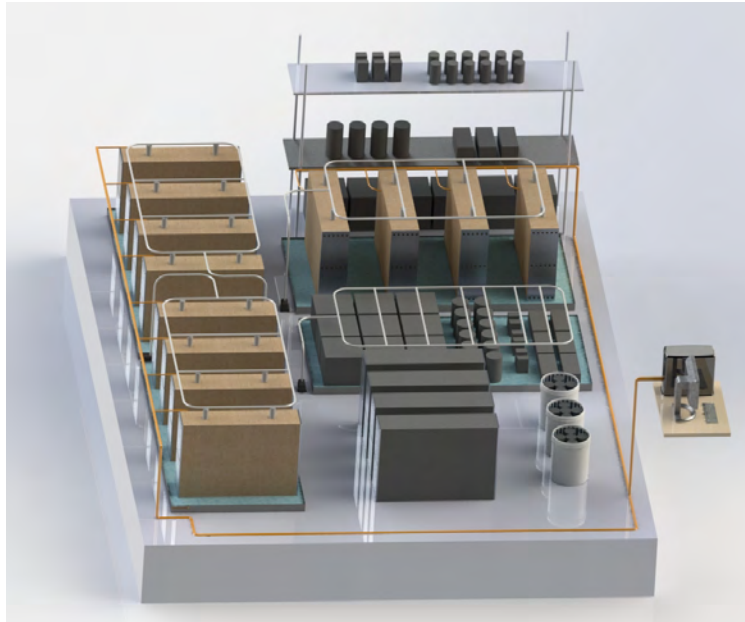


Figure 2.13: Installation of reactive and non-reactive specimens in the fog room and computer for data logging

A forklift was used to place the blocks into the pans, Fig. 2.14. Once in the pans, the blocks could be slid by hand to their proper location. All smaller specimens were carried into the room by hand.



Figure 2.14: Placing shear specimen in fog room with forklift

To prevent leaching of alkalinity from the concrete, shear specimens and blocks are wrapped in burlap

and wetted with a 1M aqueous sodium hydroxide (NaOH) solution. All the samples (except the cylinders, prisms, and wedge splitting test specimens) are placed in the 96" x 48" x 3" steel pans containing the sodium hydroxide which is pumped to the top of the concrete, Fig. 2.15(a).

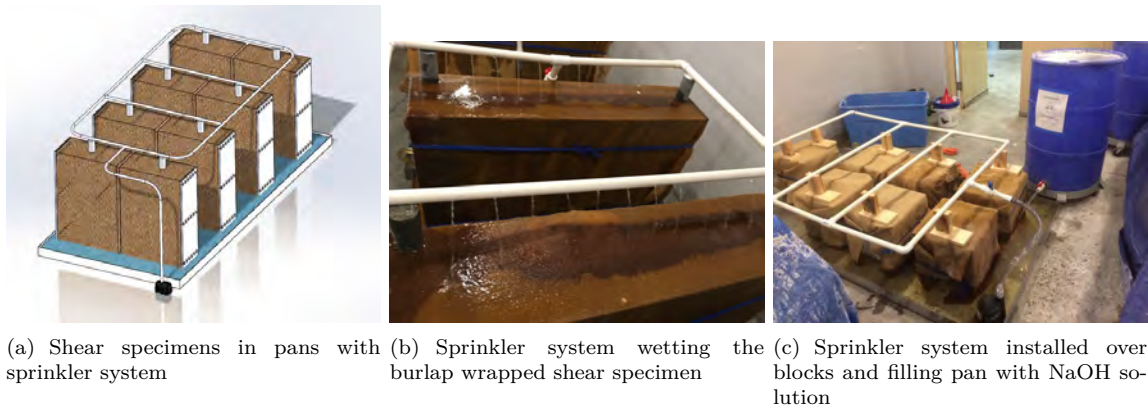


Figure 2.15: Sprinkler system for the specimens

Initially, salt water fish tank pumps were used to pump sodium hydroxide through the PVC system. These pumps were unreliable in providing a constant flow of solution. Additionally, there was a significant loss of solution due to splashing off of the specimens and out of the pans. To mitigate these problems, sump pumps shown in Figure 2.16 are utilized and prove to be much more reliable. However, since sump pumps are not designed to run continuously, they are connected a timer that turns the pumps on every 1.5 hours for three minutes. This is a sufficient amount of time to keep the burlap wet. To prevent splashing, the samples and sprinkler systems are cover in a tarp with the edges tucked into the pans.



Figure 2.16: Sump pumps used to power sprinkler system

The NaOH solution is carried through PVC pipe, which is not reactive with sodium hydroxide, where it is sprayed across the top through holes drilled into the pipe. To provide constant pressure at each spray point, the piping system is constructed in a loop across the samples using PVC tees and 90° elbows. This way, each specimen will have multiple spray points across its top face to ensure sufficient wetting. Additionally, the specimens are wrapped in a burlap fabric so it is saturated with NaOH and holds liquid against the concrete

surface. The liquid is collected in the steel pans where the process is repeated.

2.5 Expansion Measurements

As testing could not proceed until sufficient expansion took place, length change were measured along directions shown in Fig. 2.17(a). Those points were marked on the newly cast specimens, Fig. 2.17(b). Demec (demountable mechanical strain gauge) disk markers epoxy placed (special epoxy that had to resist high temperature, humidity and alkalinity), Fig. 2.17(c). Expansion was measured with the device shown in Fig. .

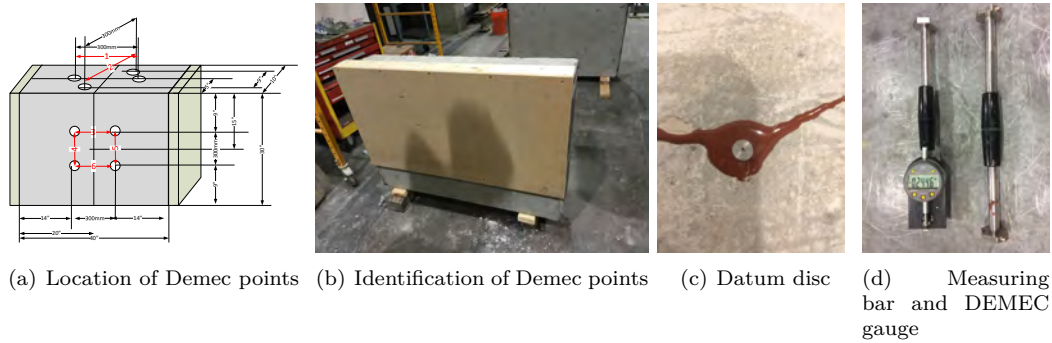


Figure 2.17: Expansion measurements

Expansion measurement for the shear and other specimens are separately reported (Saouma et al., 2016).

This page intentionally left blank.

Part II

Testing Protocol

This page intentionally left blank.

3— Pre-Mortem

It is of the utmost importance that a well defined testing protocol be specified for the various stages of the testing. Hence, three separate protocols will be specified:

Pre-mortem to address all operations from the moment the specimen is taken out of the fog room until it is installed in the testing machine.

Testing of the specimen, Chapter 4.

Post-mortem will specify how to examine the specimen and prepare the data file with the results, Chapter 5.

3.1 From Fog Room to Testing Machine

3.1.1 Specimen Removal

Specimen should be removed no earlier than five days before the test. While specimen is in the laboratory it should be covered with burlap saturated with 1M NaOH.

The night prior to installation, the burlap shall be removed, and specimen allowed to dry.

3.1.2 Notch

Once the burlap has been removed, a $\frac{1}{4}$ " cut will be made along the top and bottom of the specimen corresponding to the edge of the internal pad transmitting the vertical forces. The notch shall be at 4" from the center line as shown in Fig. 1.2. Cuts will not be made along the sides of the concrete panel which include along the centerline.

3.1.3 Splitting Tensile Strength

The concrete cylinders corresponding to the mix of the specimen shall be retrieved no earlier than a week from the test, allowed to dry for no more than 24 hrs, and then tested in the 110-kip.

Preference shall be given to conducting "brazilian test" to determine the Splitting Tensile Strength (**astm-496**).

Then consideration should be given to perform compressive strength test, (ASTM, C39, 2016).

3.1.4 Mark the Specimen

Prior to installation, and once the specimen is sufficiently dry, it should be tagged with its ID according to T-xx-S-yy-B-zz where xx is the sequential test number (1-16), yy the specimen ID (1-16) from Table 2.1,

zz the batch number (1-4).

3.2 Installation Procedure

3.2.1 Nomenclature

Installation procedure of the specimen will make reference to terms which understanding is important to avoid accidents. Those are defined next and some of them shown in Fig. 3.1.

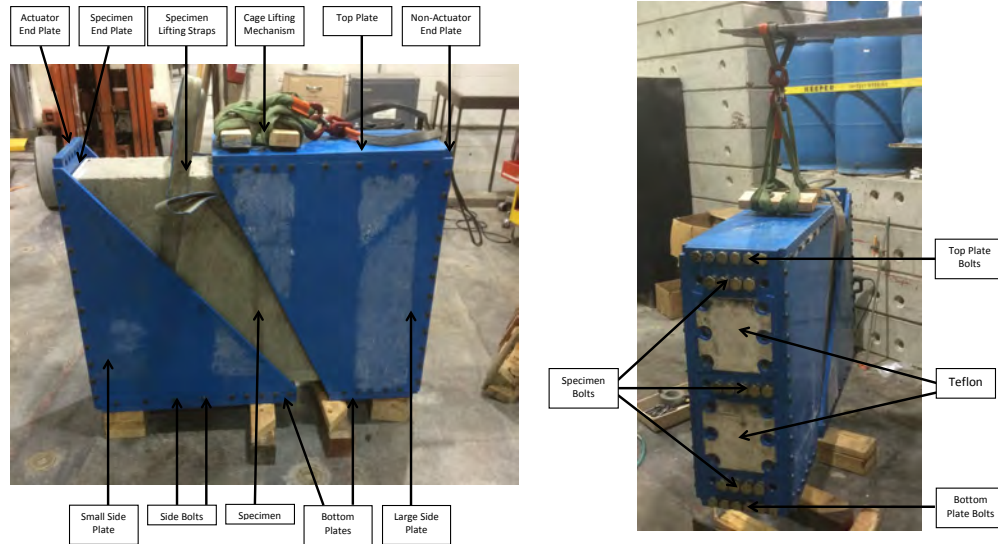


Figure 3.1: Specimen description

Actuator Clevis Bracket Squared yellow bracket that attaches to the actuator side plate with clevis bracket bolts.

Actuator End Plate Blue end plate to which the bottom plate, small side plates, and specimen are connected. The Teflon on this end plate faces towards the actuator (west) when loaded into the testing machine.

Bottom Plates Blue plates on bottom of the cage. Connected to side plates using side bolts and end plates using bottom plate bolts.

Bottom Plate Bolts Bolts connecting the end plates to the bottom plates. (Insert Bolt Size)

Cage General term referring to all blue plates when connected together. Cage consists of top plate, large side plates, small side plates, bottom plates, actuator end plate, and non-actuator end plate. Cage pieces will be referred to as “triangular cage” and “trapezoidal cage” for the actuator and non-actuator side of the cage, respectively.

Cage Lifting Mechanism Mechanism that lifts the entire cage and specimen to be loaded into the testing machine. 2x4 blocks are through bolted to the bolt holes in the top plate. Straps are wrapped around the blocks and wrapped around the forks for the fork lift.

Clevis Bracket Bolts Bolts used to connect the yellow clevis brackets to the end plates. (Insert bolt size)

Large Side Plate Trapezoidal shaped blue side plate that is connected to the top plate, bottom plate, and non-actuator side plate

Non-Actuator Clevis Bracket Rounded yellow bracket that attaches to the non-actuator side plate with clevis bracket bolts.

Non-Actuator End Plate End plate to which the top plate, bottom plate, small side plates, and specimen are connected. The Teflon on this end plate faces away from the actuator (east) when loaded into the testing machine.

Side Bolts Bolts connecting the side plates to the top plate, side plates, and bottom plates. (Insert Bolt Size).

Small Side Plate Triangular shaped blue side plate that is connected to the bottom plate and actuator side plate.

Specimen Concrete specimen that is installed into the cage to be tested. When the specimen is installed in the cage, the two together are also referred to as the specimen.

Specimen Bolts Bolts that connect the blue end plates to the specimen. (Insert Bolt Size)

Specimen Lifting Straps Flat straps that wrap under the specimen used to load the specimen into the cage. Straps are left in cage during testing.

Specimen End Plates Steel plates connected to the concrete specimen. Specimen end plates have steel studs embedded into the concrete specimen.

Teflon White material on end plates. Teflon should always be facing outwards and should be visible when the specimen is loaded into the cage.

Testing Machine Million Pound MTS testing machine located in the CU Boulder Structures Lab.

Top Plate Bolts Bolts connecting the end plates to the bottom plates. (Insert Bolt Size)

3.2.2 Checklist

The installation procedure is the results of three different methods that were evaluated. Procedures for loading shear specimens into million pound machine

1. Assemble each side of the cage on lab floor as shown in the pictures and drawings. Ensure that all bolts can be started by hand for at least one full turn before tightening with a tool. Starting bolts by hand will ensure that bolts are not mis-threaded. Do not install the top plate. Additionally and importantly, do not completely tighten any of the bolts until all the bolts (both cage and specimen) have been started. This allows movement in the cage pieces that will allow all bolts to be started.
2. Cage should be assembled on blocking (use 4x4 minimum blocking) and a minimum of two blocks should be used under each half of the cage. The trapezoidal side may require extra stabilization due to its top-heavy shape.
3. Using the specimen lifting straps (wrapped under the specimen), spreader bar, and forklift (or roof crane), lower the concrete specimen into the assembled cage. Continue to support the specimen until all the bolts have been started. Due to the specimen bolt head size and bolt hole spacing, specimen bolts should be inserted starting from one side of the bolt pattern to the other (left to right or vice versa). When tightening a bolt, the edge of the adjacent bolt heads must be vertical to allow the bolt to turn without catching on the adjacent bolt.
4. Install the top plate into the cage either by hand or using the lifting mechanism. A rubber mallet may be required to get it into position. Once all bolts have been started by hand, use wrenches or ratchets to tighten all bolts.
5. In preparation of loading the specimen and cage into the testing machine, raise the crosshead to its highest position. Additionally, wrap each steel column with the rubber mats and secure in place with

bungee cords. Ensure that the actuators have been retracted enough so that the cage and specimen can be lowered into position.

6. Using the lifting mechanism and the forklift, lift the entire specimen and cage from the blocks. With the specimen close to the floor, approach the testing machine at an angle from the northwest to the southeast. Ensure that the trapezoidal portion of the cage will enter the machine first so it will face the non-actuator side when fully installed.
7. Drive the forklift forward so the specimen goes in between the northeast and southeast column. Once the cage has cleared the northwest column, turn the specimen by hand so that it is parallel steel rods. Lower the cage and specimen until it is approximately lined up with the bolt holes on the clevis brackets, Fig. 3.2.



Figure 3.2: Specimen and cage about to be installed

8. With the specimen still supported by the forklift, use a crowbar or long bolt to rotate the round clevis brackets so the bracket face is vertical. Move the specimen with the forklift so that it sits flush and centered against the clevis brackets. Attach specimen to the clevis brackets using eight (8) clevis bracket bolts. Do not fully tighten the bolts until all clevis bracket bolts have been started.
9. At this point, the actuator side of the specimen can continue to be supported using the forklift, the specimen straps and a hand crane mounted to the cross head, or with blocking.
10. Ensure that all actuator bolts have been loosened. Place a 2x4 that is long enough to span between the top and bottom actuator on either side of the actuators. Wrap a strap around the middle of the 2x4's, between the two actuators. Wrap flat straps around the two steel columns of the non-actuator side of the testing machine at roughly the same height as the 2x4 straps. Connect the two straps on each side of the testing machine with a come-along and tighten until there is enough tension that the

2x4's will not fall. Tighten both come-alongs at the same rate so that the actuators are drawn to the specimen evenly and do not bind.

11. While the actuators are being drawn to the specimen, use a crowbar or long bolt to rotate the actuator clevis brackets so the bracket face is vertical and parallel to the specimen.
12. When the actuators are in position so the clevis brackets are flush against the specimen, connect the clevis brackets to the specimen with eight (8) clevis bracket bolts. When all clevis bracket bolts on the actuator side of the specimen have been started, then all clevis bracket bolts can be tightened. These bolts will be removed before the test begins so they do not have to be fully tightened. The bolts should have a minimum of (3) three full turns into the cage end plates to ensure proper specimen support. When the specimen can be fully supported by the clevis bracket bolts, release whatever is supporting the actuator side of the specimen.
13. Ensure that the specimen is centered in the testing machine. These procedures have been developed so that the non-actuator clevis bracket does not move during the specimen installation/removal process. However, the position of the specimen should be checked every time in case the brackets have moved during the previous test.
14. Once the position of the specimen is correct, tighten the actuator bolts. This should be done using a 3-foot pipe extension on the wrench to ensure that the actuators do not move during the test.
15. Install the roller and roller plate on the top and bottom of the specimen. The bottom roller sets in the groove of the roller plate. The top roller sits directly on top of the cage, centered on the specimen. The roller plate sits on top of the roller with the roller in the groove. Use small wooden wedges to keep the roller in place until the cross head is lowered and keeps it in place. Certify that both rollers are centered on the specimen.
16. Extend the actuators to provide enough confining pressure to keep the specimen in place. The bottom roller should be raised until it is in contact with the bottom of the cage to fully support the specimen. Once the specimen is stabilized, remove the sixteen (16) clevis bracket bolts.
17. Lower the cross head so that it levels the top roller plate. Ensure that the roller is still centered on the cage once top roller plate has been leveled.
18. Reference the Million Pound Machine Operating Procedures document to perform the loading and data recording for the test.
19. Once the test is complete and the specimen has broken, support the specimen so that it is stable and will not fall once the confining pressure is released. Since it is uncertain how the specimens will break and to what extent the two halves will be separate, the exact procedure to achieve this will be determined at the time of the test. The main goal is to keep the specimen and cage supported and together so it can be lifted out of the machine as one unit. This can be done by one or more of the following:
 - (a) Replace clevis bracket bolts
 - (b) Place blocking under each half of the specimen
 - (c) Place ratchet straps around the specimen and cage to keep separate pieces together
 - (d) Support specimen and cage with straps connected to two (2) 1-ton cranes connected to the underside of the crosshead.
 - (e) Support the specimen and cage with straps connected to the forklift
20. Once the cage and specimen are stable and confining pressure has been released, reattach the cage lifting mechanism to the cage and lift with the forklift out of the testing machine.

21. Place specimen on blocking as described in Step 2. Carefully remove support from the forklift and strapping so the specimen remains stable.
22. Remove the top plate bolts and top plate side bolts to release the top plate from the rest of the cate. Use the forklift to remove the top plate with the lifting mechanism.
23. Remove specimen bolts to release the specimen pieces from the cage. Use the specimen lifting straps and any other lifting mechanism required to remove the broken specimen from the cage and place where the end plates can be extracted from the concrete.

3.3 Pre-Tests Pictures

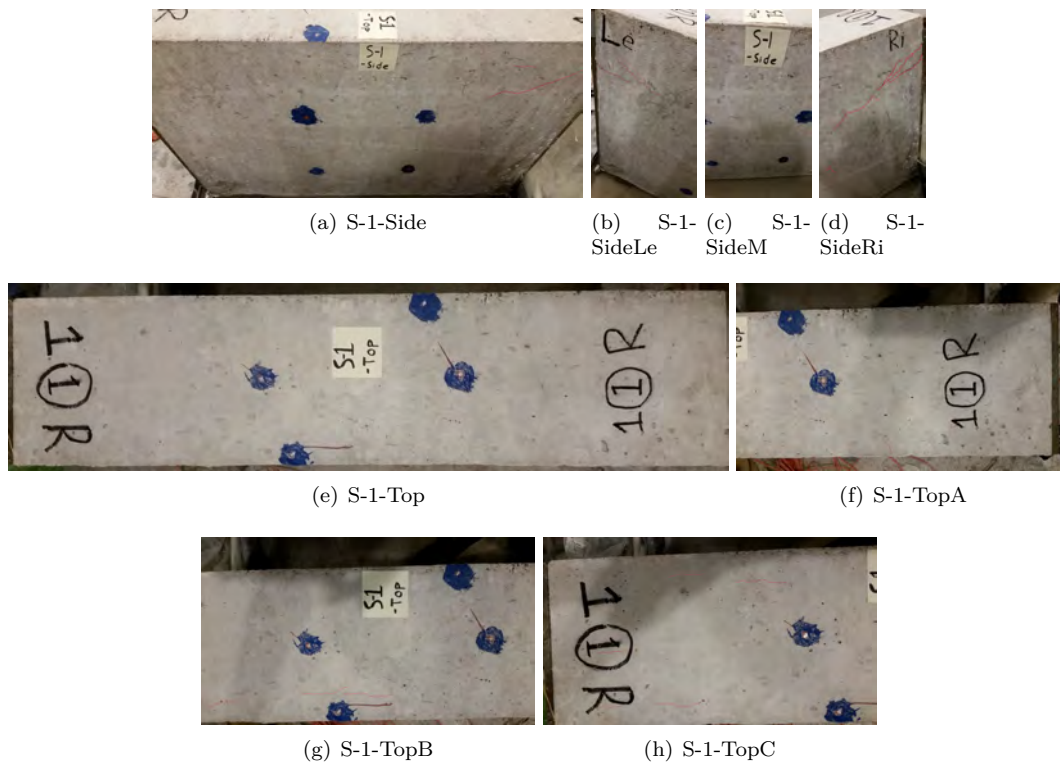


Figure 3.3: S1

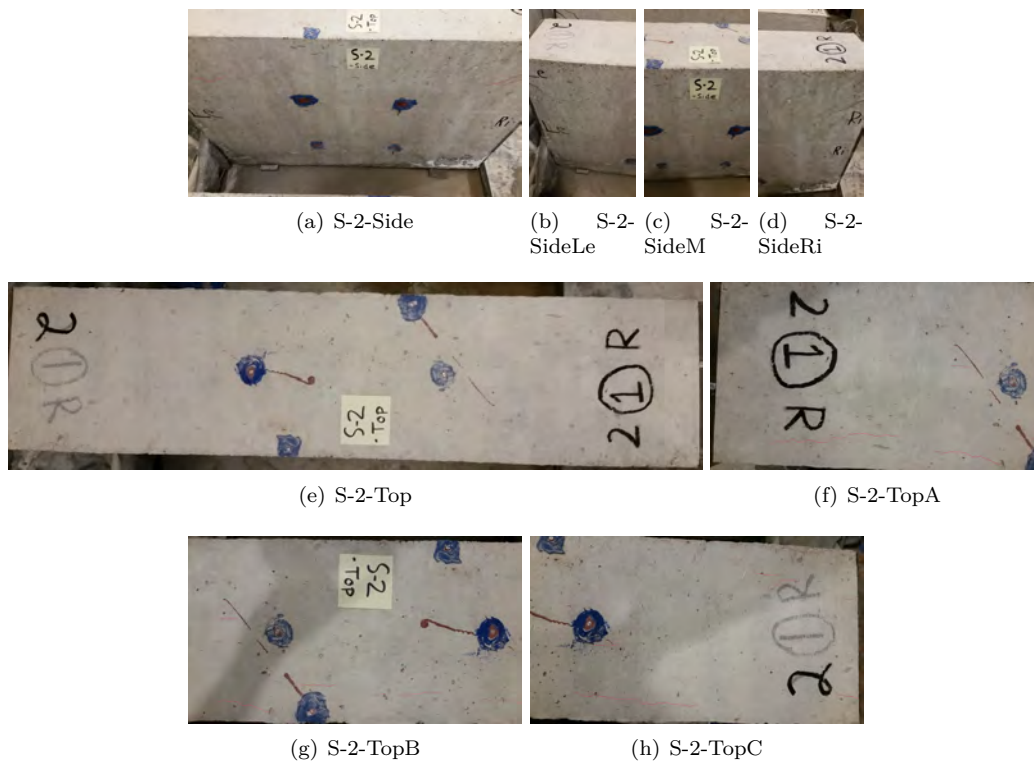


Figure 3.4: S2

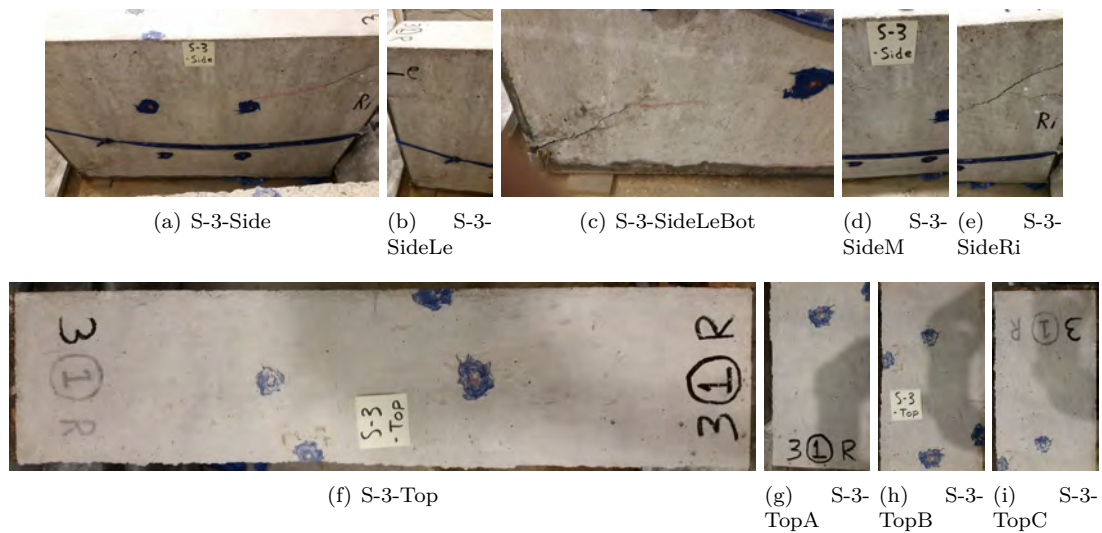


Figure 3.5: S3

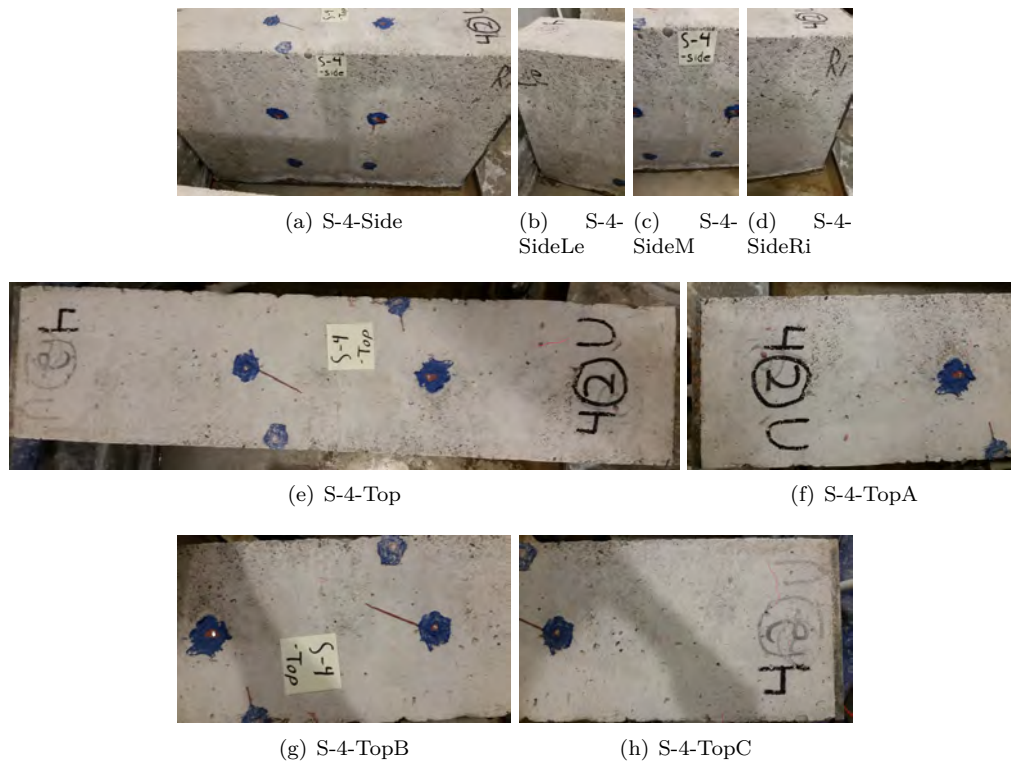


Figure 3.6: S4

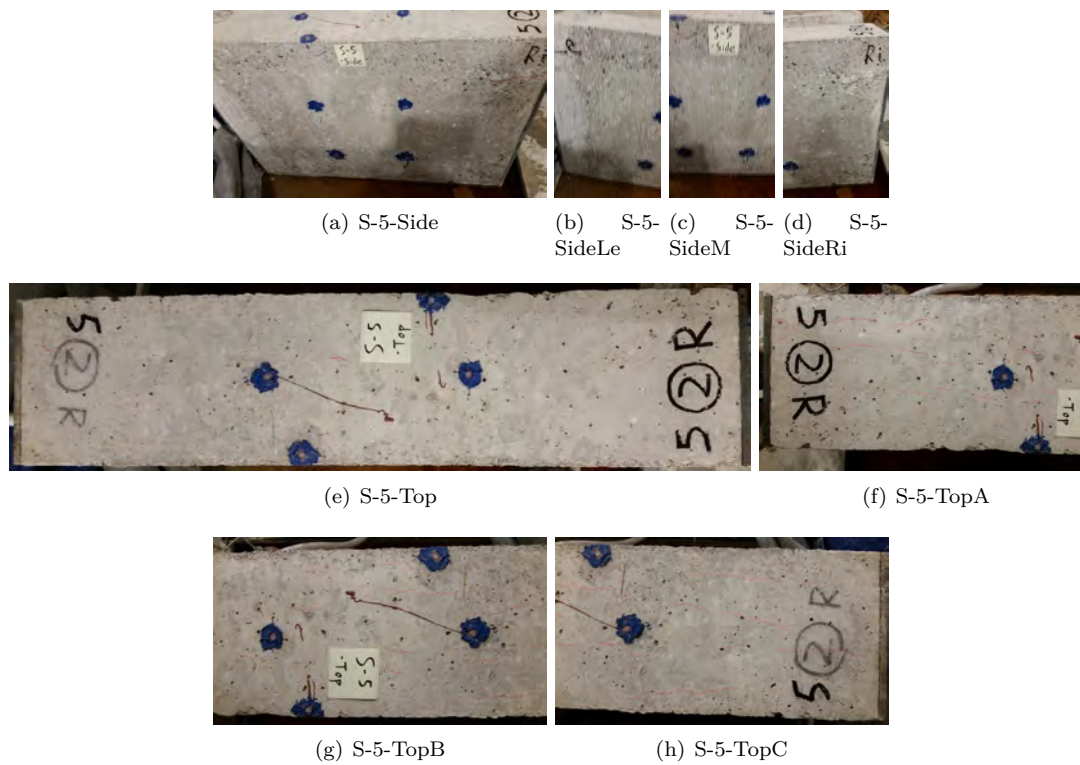


Figure 3.7: S5

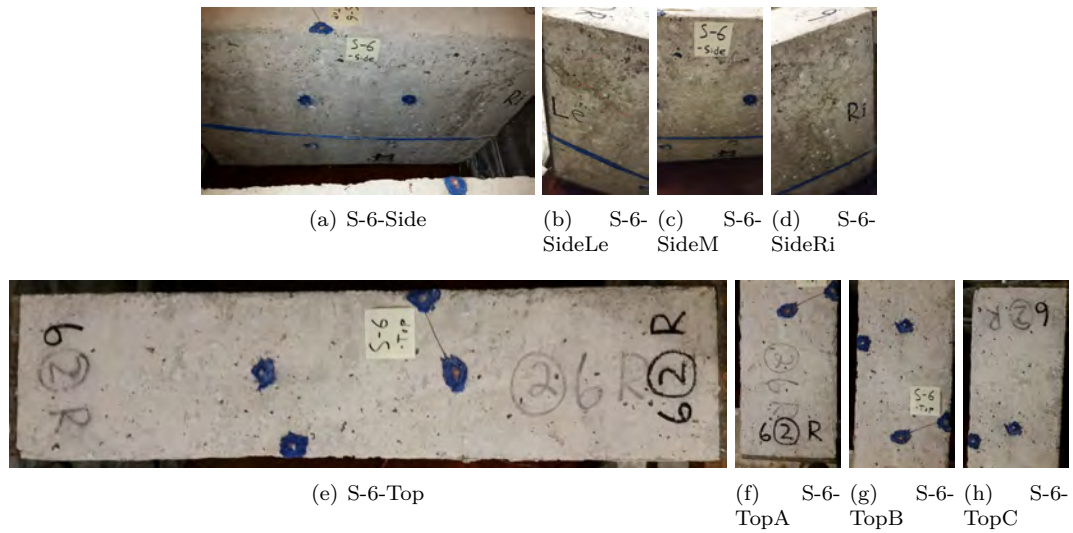


Figure 3.8: S6

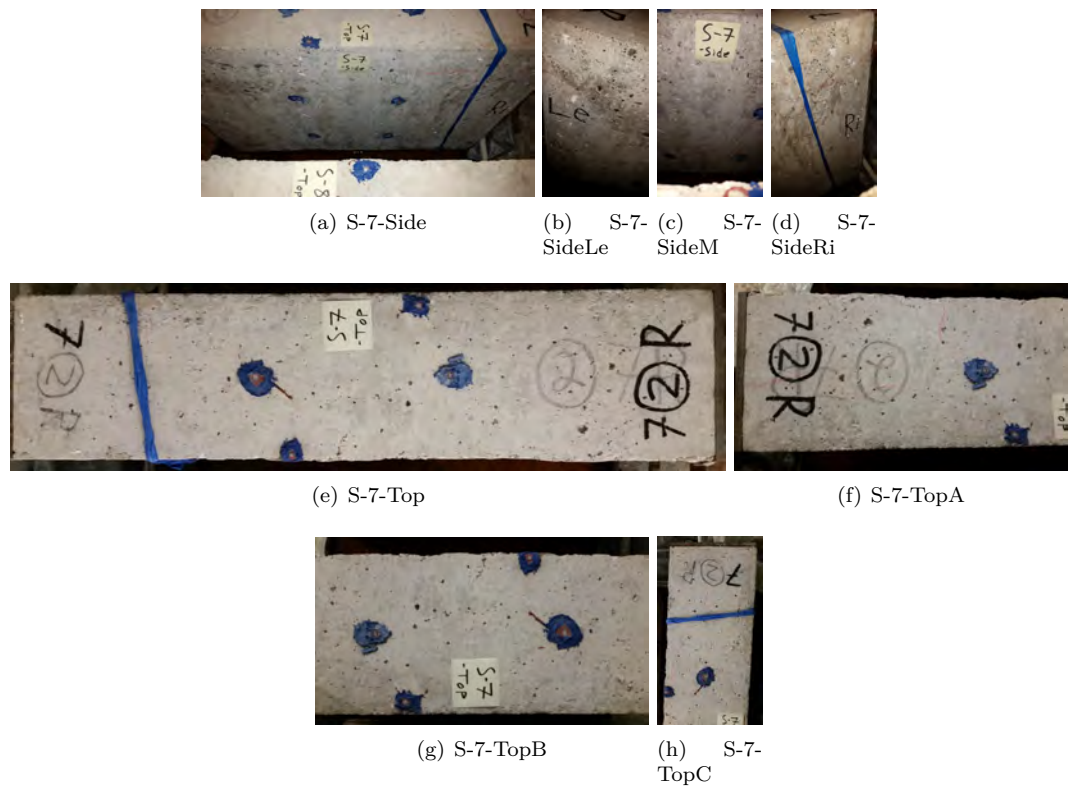


Figure 3.9: S7

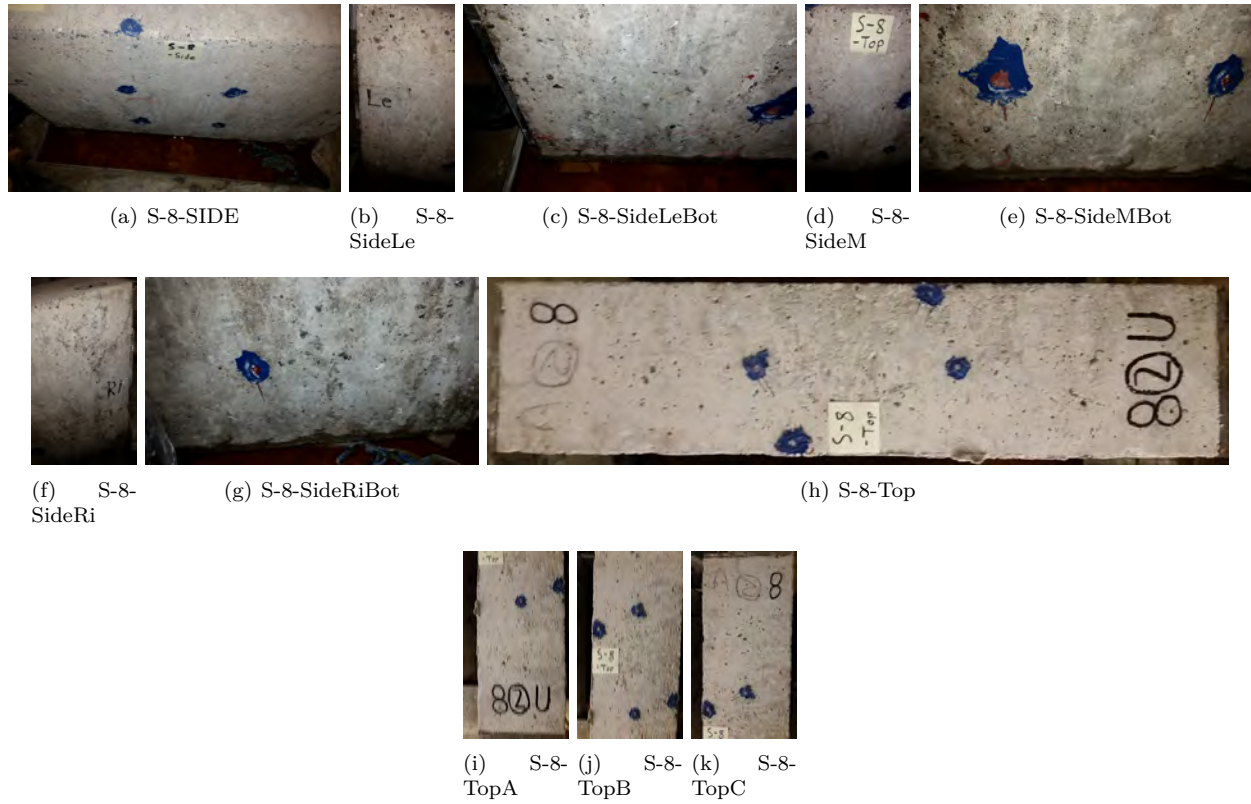


Figure 3.10: S8

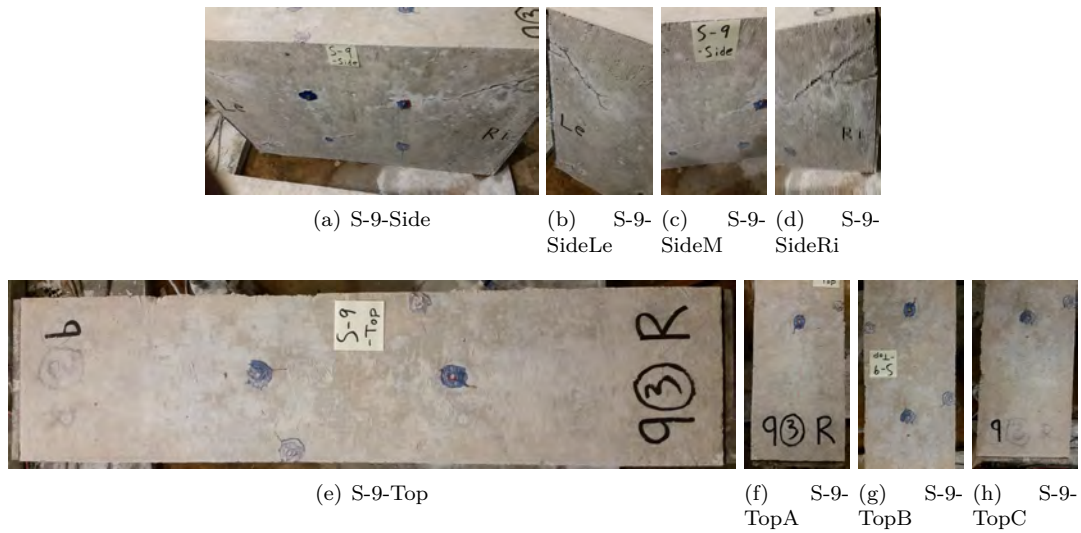


Figure 3.11: S9



Figure 3.12: S10



Figure 3.13: S11

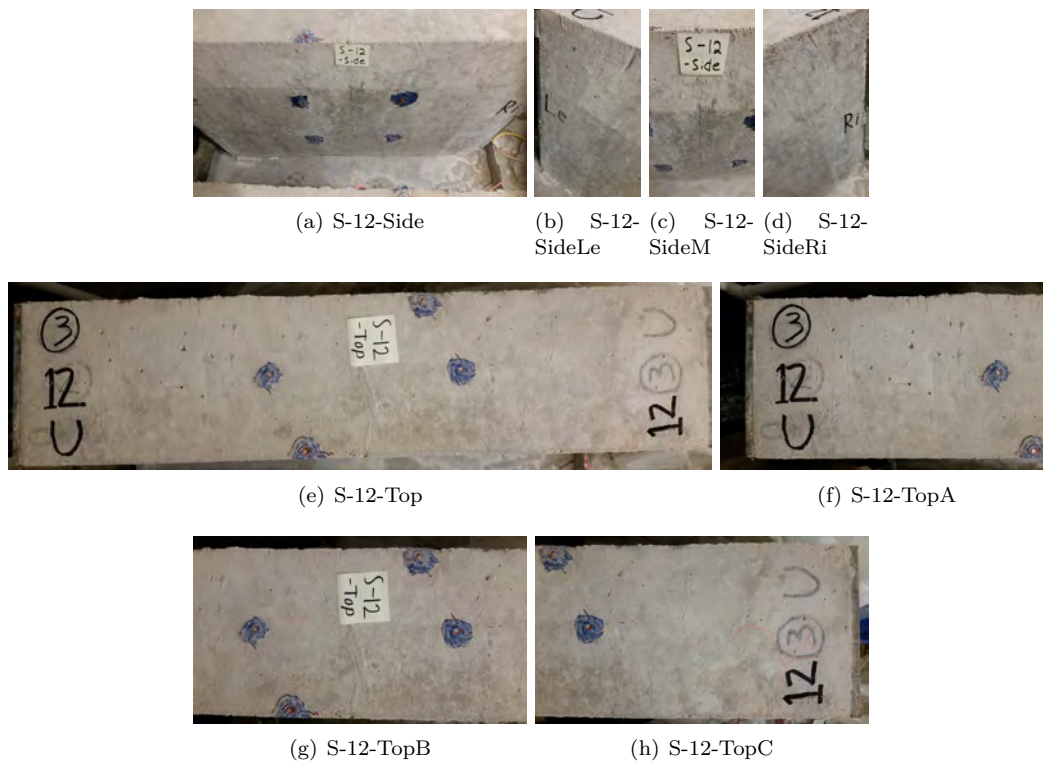


Figure 3.14: S12

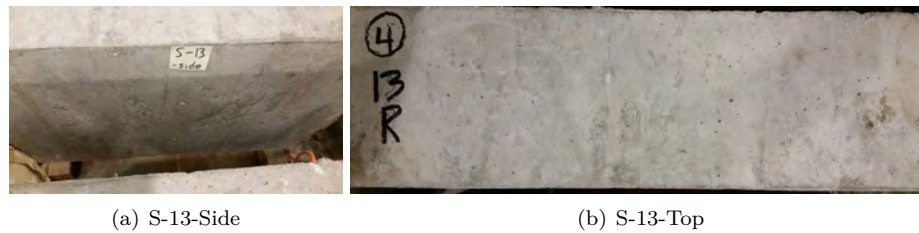


Figure 3.15: S13

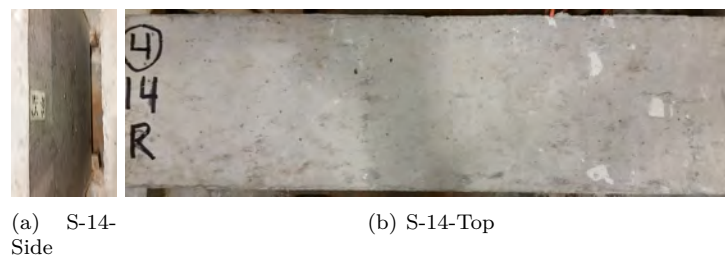


Figure 3.16: S14



Figure 3.17: S15



Figure 3.18: S16

3.4 Concrete Properties

3.4.1 Compressive Strength

Compressive strengths were measured at 7 and 28 days, Table 3.1. No cores were available to test after one year.

Table 3.1: Measured compressive strengths at 7 and 28 days

| Label | id | Batch | Diam | fc 7 | | fc 28 | | Temp | Storage | Spec Number | f _c |
|-------------|----|-------|------|------|-----|------------|-----|------|---------|-------------|----------------|
| | | | | Mean | NSD | Mean | NSD | | | | |
| 1-S-F-A-C-1 | 10 | 1 | 4 | 2.6 | 0.9 | 6.0 | 0.1 | 90 | Air | 1 | 2.9 |
| 2-S-F-A-C-1 | 14 | 2 | 4 | 4.1 | 0.2 | 5.0 | 0.1 | 90 | Air | 1 | 2.8 |
| 2-S-F-A-C-2 | 15 | 2 | 4 | 4.1 | 0.2 | 5.0 | 0.1 | 90 | Air | 2 | 1.6 |
| 3-L-F-A-C-1 | 17 | 3 | 6 | 3.7 | 0.1 | 4.2 | 0.3 | 90 | Air | 1 | 2.4 |
| 3-S-F-A-C-1 | 20 | 3 | 4 | 3.7 | 0.1 | 4.2 | 0.3 | 90 | Air | 1 | 2.3 |
| 3-S-F-A-C-2 | 21 | 3 | 4 | 3.7 | 0.1 | 4.2 | 0.3 | 90 | Air | 2 | 2.5 |
| 4-L-F-A-C-1 | 23 | 4 | 6 | 4.8 | 0.2 | 5.7 | 0.2 | 90 | Air | 1 | 3.5 |
| 4-S-F-A-C-1 | 27 | 4 | 4 | 4.8 | 0.2 | 5.7 | 0.2 | 90 | Air | 1 | 4.7 |
| 4-S-F-A-C-2 | 28 | 4 | 4 | 4.8 | 0.2 | 5.7 | 0.2 | 90 | Air | 2 | 2.4 |
| 4-S-F-A-C-3 | 29 | 4 | 4 | 4.8 | 0.2 | 5.7 | 0.2 | 90 | Air | 3 | 4.5 |
| 4-L-L-A-C-1 | 34 | 4 | 6 | 4.8 | 0.2 | 5.7 | 0.2 | 70 | Air | 1 | 3.5 |

| | | | | | | | | | | | |
|-------------|----|---|---|-----|-----|------------|-----|----|-------|---|------------|
| 1-S-F-N-C-2 | 6 | 1 | 4 | 2.6 | 0.9 | 6.0 | 0.1 | 90 | Na2OH | 2 | 2.0 |
| 3-L-L-N-C-1 | 32 | 3 | 6 | 3.7 | 0.1 | 4.2 | 0.3 | 70 | Na2OH | 1 | 2.3 |

3.4.2 Splitting Tensile Strength

Splitting tensile strength were measured a year after casting, Table 3.2

It should be noted that some specimens were stored in the fog room, other in the laboratory. Likewise, some were in an NaOH solution, others in air.

3.4.3 Measured f_c f_t relationships

. Interestingly, it was observed that there is a $\approx 50\%$ reduction in tensile strength caused by AAR, Fig. 3.19.

Table 3.2: Splitting Tensile Strengths (psi)

| Label | id | Batch | Diam | T [oF] | Storage | Spec. | f t | Mean | NSD | Mean | STD | Used | |
|---------------|----|-------|------|--------|---------|-------|-----|------|-------|------|--------|-------|-------|
| 1-S-F-A-T-1-a | 9 | 1 | 4 | 90 | Air | a | 435 | | | 432 | 4.93 | 0.430 | |
| 1-S-F-A-T-1-b | 9 | 1 | 4 | 90 | Air | b | 428 | 432 | 1.1% | | | | |
| 1-S-F-N-T-1-a | 3 | 1 | 4 | 90 | Na2OH | a | 566 | | | 431 | 99.81 | | |
| 1-S-F-N-T-1-b | 3 | 1 | 4 | 90 | Na2OH | b | 597 | 582 | 3.7% | | | | |
| 1-L-F-N-T-1-a | 1 | 1 | 6 | 90 | Na2OH | a | 373 | | | | | | |
| 1-L-F-N-T-1-b | 1 | 1 | 6 | 90 | Na2OH | b | 363 | 368 | 2.1% | | | | |
| 1-L-F-N-T-2-a | 2 | 1 | 6 | 90 | Na2OH | a | 552 | | | | | | |
| 1-L-F-N-T-2-b | 2 | 1 | 6 | 90 | Na2OH | b | 419 | 485 | 19.3% | | | | |
| 1-S-F-N-T-2-a | 4 | 1 | 4 | 90 | Na2OH | a | 349 | | | | | | |
| 1-S-F-N-T-2-b | 4 | 1 | 4 | 90 | Na2OH | b | 392 | 371 | 8.3% | | | | |
| 1-L-L-N-T-1-a | 30 | 1 | 6 | 70 | Na2OH | a | 342 | | | | | | |
| 1-L-L-N-T-1-b | 30 | 1 | 6 | 70 | Na2OH | b | 361 | 352 | 3.8% | | | | |
| 2-S-F-A-T-1-a | 11 | 2 | 4 | 90 | Air | a | 441 | | | 368 | 65.31 | 0.400 | |
| 2-S-F-A-T-1-b | 11 | 2 | 4 | 90 | Air | b | 290 | 365 | 29.2% | | | | |
| 2-S-F-A-T-3-a | 13 | 2 | 4 | 90 | Air | a | 436 | | | | | | |
| 2-S-F-A-T-3-b | 13 | 2 | 4 | 90 | Air | b | 397 | 417 | 6.6% | | | | |
| 2-S-F-A-T-2-a | 12 | 2 | 4 | 90 | Air | a | 311 | | | | | | |
| 2-S-F-A-T-2-b | 12 | 2 | 4 | 90 | Air | b | 334 | 323 | 5.1% | | | | |
| 2-S-F-N-T-1-a | 7 | 2 | 4 | 90 | Na2OH | a | 497 | | | 492 | 7.06 | | 0.300 |
| 2-S-F-N-T-1-b | 7 | 2 | 4 | 90 | Na2OH | b | 487 | 492 | 1.4% | | | | |
| 3-S-F-A-T-2-a | 19 | 3 | 4 | 90 | Air | a | 318 | | | 334 | 66.74 | | |
| 3-S-F-A-T-2-b | 19 | 3 | 4 | 90 | Air | b | 466 | 392 | 26.7% | | | | |
| 3-S-F-A-T-1-a | 18 | 3 | 4 | 90 | Air | a | 331 | | | | | | |
| 3-S-F-A-T-1-b | 18 | 3 | 4 | 90 | Air | b | 312 | 321 | 4.1% | | | | |
| 3-L-F-A-T-1-a | 16 | 3 | 6 | 90 | Air | a | 282 | | | | | | |
| 3-L-F-A-T-1-b | 16 | 3 | 6 | 90 | Air | b | 297 | 290 | 3.8% | | | | |
| 3-S-F-N-T-1-a | 8 | 3 | 4 | 90 | Na2OH | a | 291 | | | 297 | 43.76 | | |
| 3-S-F-N-T-1-b | 8 | 3 | 4 | 90 | Na2OH | b | 360 | 326 | 15.0% | | | | |
| 3-L-L-N-T-1-a | 31 | 3 | 6 | 70 | Na2OH | a | 266 | | | | | | |
| 3-L-L-N-T-1-b | 31 | 3 | 6 | 70 | Na2OH | b | 270 | 268 | 1.0% | | | | |
| 4-S-F-A-T-1-a | 24 | 4 | 4 | 90 | Air | a | 717 | | | 681 | 130.47 | 0.681 | |
| 4-S-F-A-T-1-b | 24 | 4 | 4 | 90 | Air | b | 747 | 732 | 2.9% | | | | |
| 4-S-F-A-T-2-a | 25 | 4 | 4 | 90 | Air | a | 750 | | | | | | |
| 4-S-F-A-T-2-b | 25 | 4 | 4 | 90 | Air | b | 850 | 800 | 8.8% | | | | |
| 4-S-F-A-T-3-a | 26 | 4 | 4 | 90 | Air | a | 772 | | | | | | |
| 4-S-F-A-T-3-b | 26 | 4 | 4 | 90 | Air | b | 640 | 706 | 13.3% | | | | |
| 4-L-F-A-T-1-a | 22 | 4 | 6 | 90 | Air | a | 753 | | | | | | |
| 4-L-F-A-T-1-b | 22 | 4 | 6 | 90 | Air | b | 666 | 709 | 8.6% | | | | |
| 4-L-L-A-T-1-a | 33 | 4 | 6 | 70 | Air | a | 443 | | | | | | |
| 4-L-L-A-T-1-b | 33 | 4 | 6 | 70 | Air | b | 476 | 459 | 5.1% | | | | |

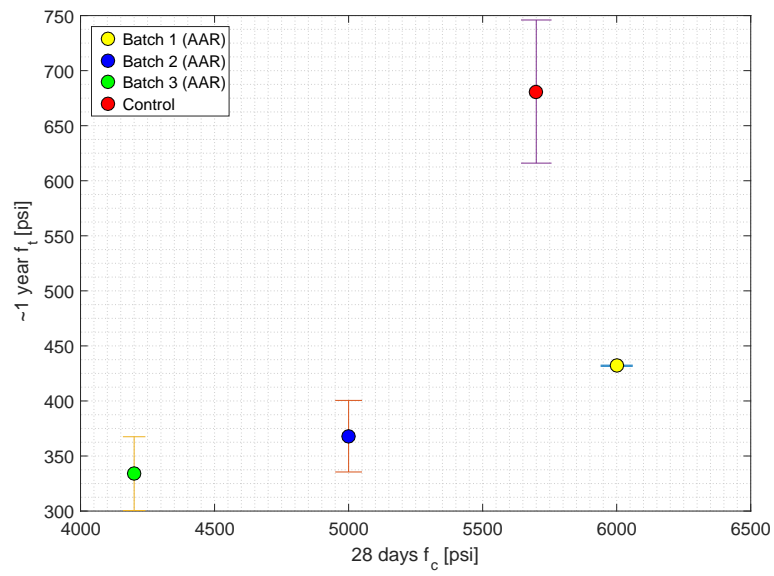


Figure 3.19: Compressive *vs* tensile splitting strengths

4— Testing

4.1 Test Preparation

4.1.1 Equipment preparation

A basic understanding of the MTS million-pound controller, hydraulic actuator operation, LabVIEW, and electrical sensor connections is necessary to be successful with this procedure. The cart with the National Instruments PXI chassis from the Control Room will need to be positioned near the MTS million-pound control console to begin. The pump oil will need to be warmed up, and so the pump can be running to begin the warm-up. Make sure that the specimen is not being supported by the MTS actuator, as this actuator will need to be moved before testing. The MTS console can be powered on, but the HSM should be off while making connections.

4.1.2 Wiring connections

These connections can be made in any order. The sensor wires are neatly coiled up on the middle shelf of the computer cart. Locate each cable by name and uncoil the whole length of cable before making the connection. Many of these connections are labeled on both the wire and on the receptacle.



Figure 4.1: Connections from SCXI-1314 terminal block

1. *Valve back pressure*: Plug this circular plug (black cable) into the pressure transducer receptacle on the back side (that is, the west side) of the horizontal control manifold.
2. *Valve front pressure*: Plug this circular plug (black cable) into the pressure transducer receptacle on the front side (that is, the east side) of the horizontal control manifold, Fig. 4.2.

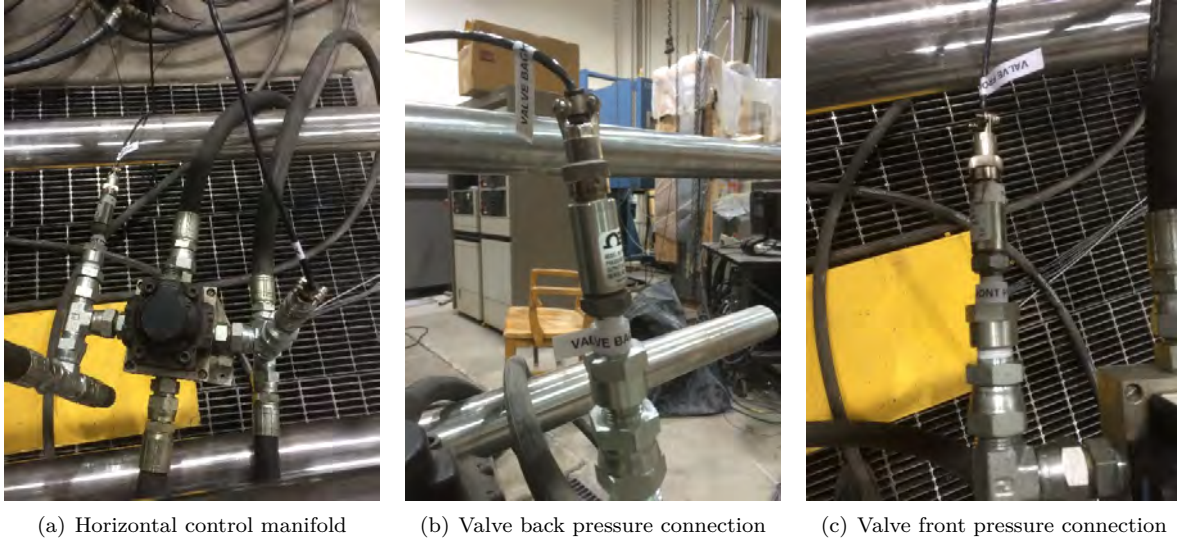


Figure 4.2: Valve front pressure connection

3. *Force and Disp*: Plug these four banana plugs (gray cable) into the sockets on the MTS control console. *Disp* (brown/white and brown wires) connects to the *Stroke module*, and *Force* (blue/white and blue wires) connects to the *Load module*. Red plugs to red sockets, and black plugs to black sockets, Fig. 4.3.



Figure 4.3: Force Displacement connections

4. *Servo valve*: Plug this circular plug (gray cable) into the servovalve receptacle of the horizontal control manifold, Fig. 4.4(a).
5. *MTS command*: Plug this circular plug (orange cable) into the *Programmer 1* socket on the back of the MTS control console, Fig. 4.4(c).
6. *HSM power cable*: Move the blue *HSM power box* to the top of the cart. Make sure both switches are in the *Off* position. Find the black coiled wire on the floor by the hydraulic service manifold. Connect

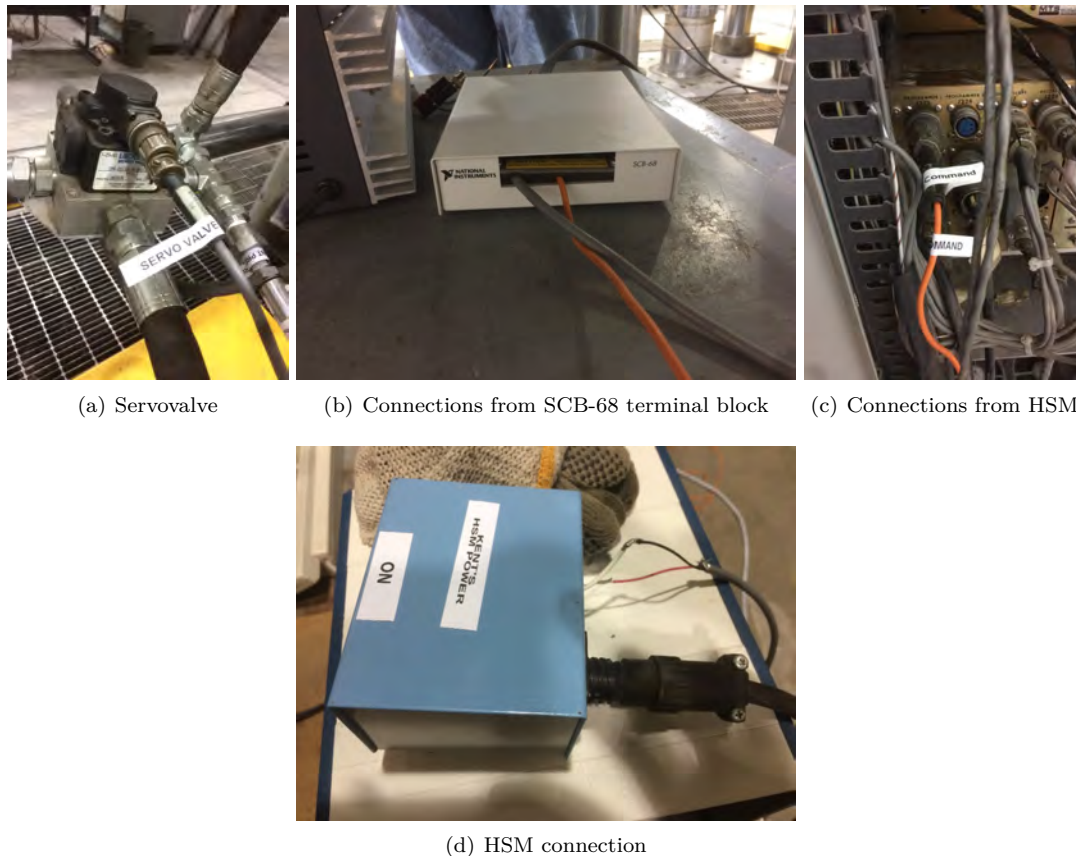


Figure 4.4: Setup details

this black wire to the back of the box, Fig. 4.4(d)

4.1.3 Position switches, start software

This section will prepare the computer and program to control the actuators.

1. Turn on the power to the MTS control console.
2. Turn on the power to the black power supply on the middle shelf of the cart.
3. Turn on the power to the National Instruments SCXI chassis on the top of the cart.
4. Turn on the power to the National Instruments PXI computer on the bottom shelf of the cart.
5. After the computer boots up, log in to Windows (see Derek or Kent for the username and password).
6. Navigate to My Documents, LabVIEW Data.
7. Check for the file **Victor Test.txt** and if it exists then rename it or delete it. This file will be overwritten by the program.
8. Navigate to My Documents, Victor NRC, FPGA Voltage Output.
9. Open the **FPGA Project.lvprog** file. This will start LabVIEW.
10. After LabVIEW opens, look in the *Project Explorer window*. Double-click the **Combined Control.vi** program. This will open the program in LabVIEW.
11. Make sure that the program's switches are all in the off position.
12. Start the program.

13. Click the Restart FPGA button and the FPGA *running* indicator should illuminate.

4.1.4 Configure the settings

Confirm or change these settings in the LabVIEW program.

1. Set the vertical loading under **Rate in/min** to **0.05**.
2. Set the horizontal **Setpoint** to **-4**.
3. Set the **Gain** to **0.005**.
4. Turn on **Pressure control**.

4.1.5 Prepare for the test

Now we will adjust the specimen and actuators so that the setup is ready for loading. Note that the MTS HSM enables the vertical actuator, and the Kent's HSM Power box enables the horizontal actuators.

1. On the MTS machine verify no DC error and then turn on the HSM to high.
2. Support the specimen with the MTS actuator by moving it up slowly using the manual control knob. Lift the specimen about $\frac{1}{4}$ inch, watching the yellow brackets to see when they become unbound. In other words, the actuator should support the specimen, not the horizontal actuators.
3. Lower the MTS crosshead onto the loading plate, take care that the rod is in contact with the blue loading cage and that the crosshead platen is contacting the square loading plate.
4. Unbolt the horizontal actuator's yellow and blue brackets.
5. Adjust the MTS actuator moving the specimen upwards or downward to remove the gap at the top to maintain a pre-load force of 100-300 lbs.
6. Turn on the horizontal actuator HSM low switch. **Caution, actuators will begin clamping!**
7. Turn on the horizontal actuator HSM high switch.
8. Wait for horizontal actuators to clamp the specimen and build up pressure, as read in the **Confinement force** reading in LabVIEW. This will take about 30 seconds.

4.2 Testing

4.2.1 LabView Operation

1. Adjust MTS actuator to apply 100-300 lbs of initial starting vertical load.
2. In LabVIEW reduce the horizontal **Setpoint** at about 1 kip per second until reaching **-88** kips.
3. In LabVIEW turn on **Record data to file**.
4. In LabVIEW turn on **Load**.
5. In LabVIEW turn on **Run**.
6. Observe the loading, watching for any problems that might arise. Occasional adjustment of the horizontal **Setpoint** might be necessary to maintain 88 kips of confinement force.
7. Movement can be paused by switching **Run** to off, and then back to on to resume.
8. When test should be stopped, turn off **Run**.
9. In LabVIEW turn off **Record data to file**.

4.2.2 Notification

During testing the operator (Kent) should shout the load at 100 kip increment.

4.2.3 Crack Identification

During the test, some cracks may become visible within the space between the blue plates. Those should be marked with a thick felt pen, and labeled sequentially with letters. Markers at the tip of the visible tip should indicate the corresponding load.

4.3 Test Termination

4.3.1 Safe the Specimen

Now we'll get things stabilized so that the specimen will stay put and be ready for removal.

1. In LabVIEW set the vertical loading under **Rate in/min to 1**.
2. In LabVIEW turn off **Load**.
3. In LabVIEW turn on **Run**. Wait for the vertical force to drop to about 40 kips, then set the horizontal **setpoint** to **-4** to lessen the compression on the specimen.
4. Wait for the vertical actuator to lower back to the starting position. The specimen should slide down without leaving a gap between the specimen and actuator.
5. If there is a gap at the bottom, then change the horizontal **Setpoint** to **+10** which will open the horizontal actuators and drop the specimen.
6. Raise the crosshead.
7. Support the specimen with blocks, the forklift, etc.
8. Unbolt the horizontal actuators from the tension rods.
9. Extend the horizontal actuators by setting horizontal **Setpoint** to **-100**.
10. Retract the horizontal actuators by setting horizontal **Setpoint** to **+100**.
11. Wait for the actuators to retract completely.
12. Turn off the horizontal HSM high switch.
13. Turn off the horizontal HSM low switch.
14. Turn off the MTS HSM.
15. Specimen now ready for removal. Hydraulic pumps may be shut down.

4.3.2 Save data, shut down

1. Rename the **Victor Test.txt** file to today's date. This file contains the test measurements.
2. Copy that file and any testing notes off the computer.
3. Verify that the MTS HSM is off.
4. Quit the LabVIEW program.
5. Close the LabVIEW program window.
6. Close the LabVIEW project window.
7. Shut down Windows.
8. After Windows shuts down, turn off the National Instruments PXI computer on the bottom shelf of the cart.

9. Turn off the power to the National Instruments SCXI chassis on the top of the cart.
10. Turn off the power to the black power supply on the middle shelf of the cart.
11. Turn off the power to the MTS control console.

4.3.3 Unhook wires

Disconnect the cables that were connected in the beginning, taking care to coil them nicely and to stack them on the shelves of the cart where they won't fall off or disrupt other uses.

1. HSM power cable (connecting to Kent's HSM power box)
2. MTS command
3. Servovalve
4. Force and Disp
5. Valve front pressure
6. Valve back pressure

5 — Post-Mortem

5.1 Test Notes

Notes were taken by the technician following each test. Those proved to be helpful in better understanding them, however great caution should be exercised in interpreting them as at times visual observations were contradicted by recorded data.

Test 1 *Pour 1 specimen 1 reinforced: Specimen was scored around the center. Steel plates inserted between the blue cage and specimen. Vertical loading at 0.05 inches per minute. Used 88 kips of total horizontal force. Broke at 235 kips. Loaded a bit longer, did get back up to 235 kips but blue plate in contact at bottom so stopped. Unloaded to zero*

Test 2 *Pour 1 specimen 2 reinforced. Specimen was notched at top and bottom, 1/4 inch. Steel plates inserted between the blue cage and specimen. Vertical loading at 0.05 inches per minute. Used 88 kips of total horizontal force. Broke at 205 kips I think. Several bolts failed before breaking, first at 185 kips. Blue top and bottom plates were bending outwards from inner plate pressure. Unloaded to zero.*

Test 3 *Pour 1 specimen 3 reinforced. Horizontal control cable had some issues before test. Specimen was notched at top and bottom, 1/4 inch. Steel plates inserted between the blue cage and specimen. First test with vertical fasteners added to prevent bowing. Vertical loading at 0.05 inches per minute. Shear cracking starting about 170 kips. Bigger, audible cracking 195 kips. Corner cracks starting 210 kips. Second shear crack line 230 kips. Peak 237 kips, good force drop. Force drop to 210 kips, then blue plate contacted at bottom causing strengthening again. Used 88 kips of total horizontal force. Unloaded to zero.*

Test 4 *Pour 2 specimen 4 unreinforced. Horizontal control cable had some issues before test. Specimen was notched at top and bottom, 1/4 inch. Steel plates inserted between the blue cage and specimen. Second test with vertical fasteners added to prevent bowing. Vertical loading at 0.05 inches per minute. Peak at 155 kips. Quick force drop off. Used 88 kips of total horizontal force. Unloaded to zero.*

Test 5 *Pour 2 specimen 5 reinforced. Horizontal control cable had some issues before test. Specimen was notched at top and bottom, 1/4 inch. Steel plates inserted between the blue cage and specimen. Vertical loading at 0.05 inches per minute. Heard cracking at 155 kips. Shear crack visible at 197 kips. Also crack from rebar formed a little later, same opening size as shear crack. Peak at 213 kips. Used 88 kips of total horizontal force. Unloaded to zero.*

Test 6 *Pour 2 specimen 6 reinforced. Horizontal control cable replaced. Horizontal integral control added. Specimen was notched at top and bottom, 1/4 inch. Steel plates inserted between the*

- blue cage and specimen. Vertical loading at 0.05 inches per minute. Shear crack visible at 204 kips. Also crack from rebar formed a little later, same opening size as shear crack. Peak at 221 kips. Used 88 kips of total horizontal force. Unloaded to zero.*
- Test 7** *Pour 2 specimen 7 reinforced. Specimen was notched at top and bottom, 1/4 inch. Steel plates inserted between the blue cage and specimen. Vertical loading at 0.05 inches per minute. Small cracking sounds at 170 kips. Shear crack visible at 202 kips. Also crack from rebar formed a little later, same opening size as shear crack. Small cracking sounds associated with force losses 200-220 kips. Peak at 232 kips. Used 88 kips of total horizontal force. Unloaded to zero.*
- Test 8** *Pour 2 specimen 8 unreinforced. Added crack opening LVDT at 15-degree angle (perpendicular to crack), two inches below center. Specimen was notched at top and bottom, 1/4 inch. Steel plates inserted between the blue cage and specimen. Vertical loading at 0.05 inches per minute. Small cracking sounds at 150 kips. Shear crack visible at 150 kips. No crack coming from the corners this time. Peak at 159 kips. Didn't break into two halves. Used 88 kips of total horizontal force. Unloaded to zero.*
- Test 9** *Pour 3 specimen 9 reinforced. Crack opening LVDT at 15-degree angle (perpendicular to crack), two inches below center. Specimen was notched at top and bottom, 1/4 inch. Steel plates inserted between the blue cage and specimen. Started with large corner cracks. Vertical loading at 0.05 inches per minute. Shear crack visible at 188 kips. Peak at 220 kips. Used 88 kips of total horizontal force. Unloaded to zero.*
- Test 10** *Pour 3 specimen 10 reinforced. Crack opening LVDT at 15-degree angle (perpendicular to crack), two inches below center. Specimen was notched at top and bottom, 1/4 inch. Steel plates inserted between the blue cage and specimen. Started with minimal corner cracks. Vertical loading at 0.05 inches per minute. Quite large corner crack developed, many times wider than shear crack. Shear crack visible at 160 kips. Peak at 180 kips more or less, blue cage in contact with specimen changing load path. Used 44 kips of total horizontal force. Unloaded to zero.*
- Test 11** *Pour 3 specimen 11 reinforced. Repaired horizontal pressure gauge wiring. While confining, at 120 kips heard several pops and specimen seemed to move. Horizontal rods were slipping on the bottom at 120 kips, and on top at 170 kips. Goal of 176 not possible, running at 100 kips confinement. Crack opening LVDT at 15-degree angle (perpendicular to crack), one inch below center. Specimen was notched at top and bottom, 1/4 inch. Steel plates inserted between the blue cage and specimen. Started with significant corner cracks. Vertical loading at 0.05 inches per minute. Heard small cracking from corners 60+ kips. Corner cracks visibly opening 130+ kips. Shear crack visible at 200 kips. Pop and force drop at 231 kips. Peak at 241 kips more or less, blue cage in contact with specimen changing load path. Used 100 kips of total horizontal force. Unloaded to zero.*
- Test 12** *Pour 3 specimen 12 unreinforced. Crack opening LVDT at 15-degree angle (perpendicular to crack), one inch below center. Specimen was notched at top and bottom, 1/4 inch. Steel plates inserted between the blue cage and specimen. Started with minimal corner cracks. Vertical loading at 0.05 inches per minute. Shear crack visible at 70 kips. Pop and force drop at 160 kips. Peak at 160 kips. Second pop and force drop at 149 kips. Used 100 kips of total horizontal force. Unloaded to zero.*

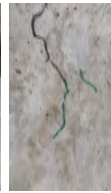
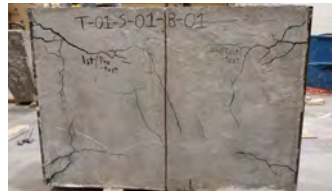
- Test 13** *Pour 4 specimen 13 reinforced. Crack opening LVDT at 15-degree angle (perpendicular to crack), one inch below center. Specimen was notched at top and bottom, 1/4 inch. Steel plates inserted between the blue cage and specimen. Started with minimal corner cracks. Vertical loading at 0.05 inches per minute. Pop and force drop at 218. Shear crack visible at 218. Second force drop at 270 kips but no pop. Peak at 286 kips. Used 88 kips of total horizontal force. Unloaded to zero*
- Test 14** *Pour 4 specimen 14 reinforced. Added strain gauges. Crack opening LVDT at 15-degree angle (perpendicular to crack), one inch below center. Specimen was notched at top and bottom, 1/4 inch. Steel plates inserted between the blue cage and specimen. Started with minimal corner cracks. Specimen damaged by accidental actuator movement. About 240 kips applied quickly with very low confinement. Small shear crack already started because of that. Vertical loading at 0.05 inches per minute. Shear crack visible at 0 kips. Corner cracking visible 250 kips. Peak at 284 kips. Used 88 kips of total horizontal force. Unloaded to zero.*
- Test 15** *Pour 4 specimen 15 unreinforced. Added strain gauges. Crack opening LVDT at 15-degree angle (perpendicular to crack), one inch below center. Specimen was notched at top and bottom, 1/4 inch. Steel plates inserted between the blue cage and specimen. Started with no corner cracks. Vertical loading at 0.05 inches per minute. Shear crack visible at 232 kips, quick failure. Peak at 235 kips. Used 100 kips of total horizontal force. Unloaded to zero.*
- Test 16** *Pour 4 specimen 16 unreinforced. Added strain gauges. Crack opening LVDT at 15-degree angle (perpendicular to crack). Specimen was notched at top and bottom, 1/4 inch. Steel plates inserted between the blue cage and specimen. Started with no corner cracks. Vertical loading at 0.05 inches per minute. Shear crack visible about 190 kips, slow failure. Peak at 197 kips. Used 88 kips of total horizontal force. Unloaded to zero*

5.2 Cracks and Pictures

Whereas some of the visible cracks during testing have been marked, additional ones will appear after the cage has been removed.



(a) S-01-B-01-Back

(b)
S-01-B-01-
Close

(c) S-01-B-01-Front



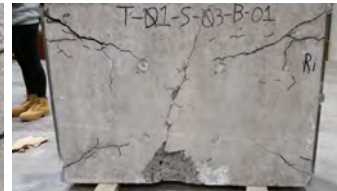
(d) S-02-B-01-Back

(e)
S-02-B-01-
Close

(f) S-02-B-01-Front



(g) S-03-B-01-Back

(h)
S-03-B-01-
Close

(i) S-03-B-01-Front



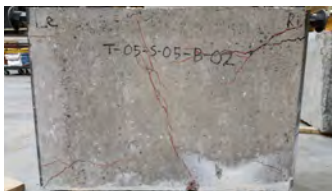
(j) S-04-B-02-Back



(k) S-04-B-02-Front



(l) S-05-B-02-Back

(m)
S-05-B-02-
Close

(n) S-05-B-02-Front



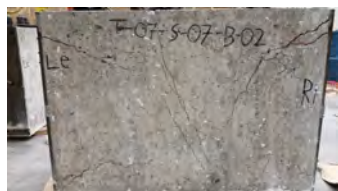
(o) S-06-B-02-Back

(p)
S-06-B-02-
Close

(q) S-06-B-02-Front



(r) S-07-B-02-Back

(s)
S-07-B-02-
Close

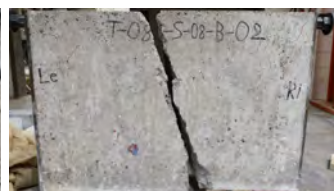
(t) S-07-B-02-Front



(u) S-08-B-02-Back



(v) S-08-B-02-Close



(w) S-08-B-02-Front



(x) S-09-B-03-Back

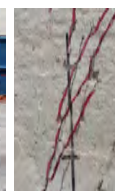
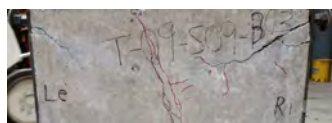
(y)
S-09-B-03-
Close

Figure 5.2: *Post-Mortem* pictures of specimens 10 to 16

This page intentionally left blank.

Part III

Test Results

6 — Test Results

6.1 Test Matrix

Table 2.1 detailed the 16 specimens cast, it is shown again in Table ?? to show the confining forces applied in each one of them and the corresponding group (explained in Fig. 6.1). Most specimens where subjected to a “base-line” confining force of 88 kips, and some where subjected to a lower or higher ones to assess their impact on the strength, Fig. 1.11. The test matrix is better visualized (and understood) through Fig. 6.1.

Table 6.1: Shear specimens cast

| Mix | ID | Reactive | Reinforcement | Conf-Force [Kips] | Group |
|-----|----|----------|---------------|-------------------|-------|
| 1 | 1 | Y | Y | 88 | A |
| | 2 | | Y | 88 | A |
| | 3 | | Y | 88 | A |
| 2 | 4 | Y | N | 88 | D |
| | 5 | | Y | 88 | A |
| | 6 | | Y | 88 | A |
| | 7 | | Y | 88 | A |
| | 8 | | N | 88 | D |
| 3 | 9 | Y | Y | 88 | A |
| | 10 | | Y | 44 | B |
| | 11 | | Y | 100 | C |
| | 12 | | N | 100 | E |
| 4 | 13 | No | Y | 88 | F |
| | 14 | | Y | 88 | F |
| | 15 | | N | 100 | H |
| | 16 | | N | 88 | G |

Eight different configurations were tested (A-G) varying:

1. Effect of AAR:
 - (a) Presence: A, B, C, D, E;
 - (b) Absence: F, G, H
2. Effect of confinements
 - (a) Base (A, D, F, G).
 - (b) Low (B).
 - (c) High (E, C, H).
3. Effects of reinforcements:
 - (a) Reinforced concrete (structural testing): A, B, C, F
 - (b) Plain concrete (Material testing): D, E, G, H

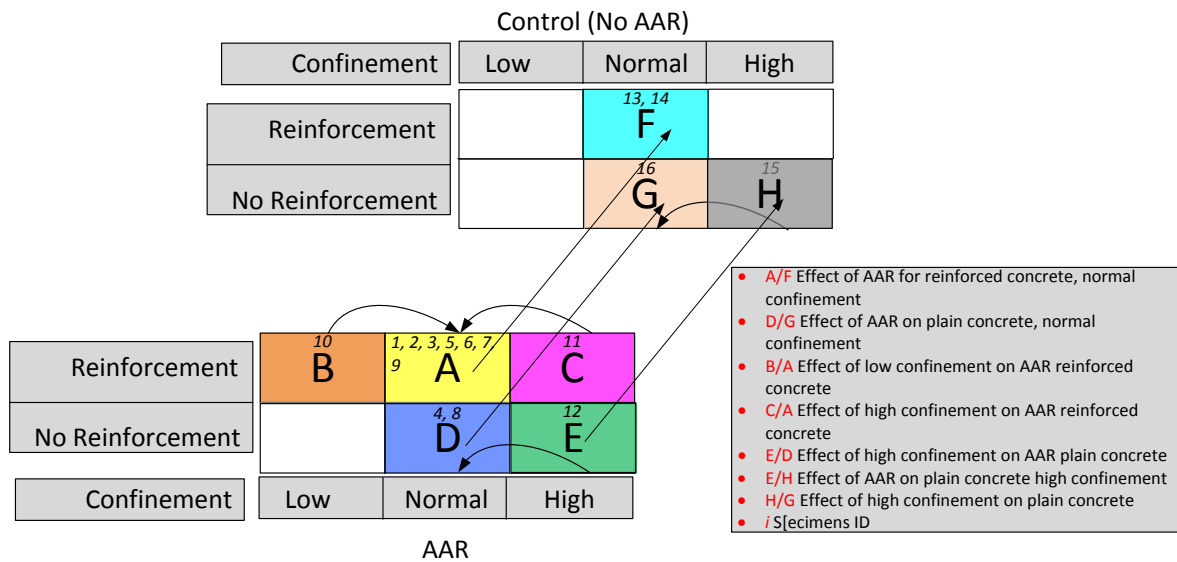


Figure 6.1: Test Matrix

Also shown in the figure are the specimens id pertaining to each group.

6.2 Analysis Strategy

For the previously defined test matrix, the following 7 questions will be investigated:

Effect of AAR on material and structural response:

1. **A-F** What is the effect of AAR on reinforced concrete (structural) subjected to base confinement?
2. **D-G** What is the effect of AAR on plain concrete (material) subjected to base confinement?
3. **E-H** What is the effect of AAR on plain concrete (material) subjected to high confinement?

Effect of Confinements under various scenarios. This will nullify (to some extent) the impact of the selected base normal traction, and confirm results if a higher confinement yields a higher failure shear force:

4. **B-A** What is the effect of low confinement on reinforced concrete with AAR?
5. **C-A** What is the effect of high confinement on reinforced concrete with AAR?
6. **E-D** What is the effect of high confinement on plain concrete with AAR?
7. **H-G** What is the effect of high confinement on plain concrete without AAR?

6.3 Expansion Measurements

To contextualize the shear strength response, it is important to have an indication of the AAR expansion they underwent prior to testing. This is shown in Fig. 6.2. It is presumed that those specimens underwent on average a 0.5% AAR expansion.

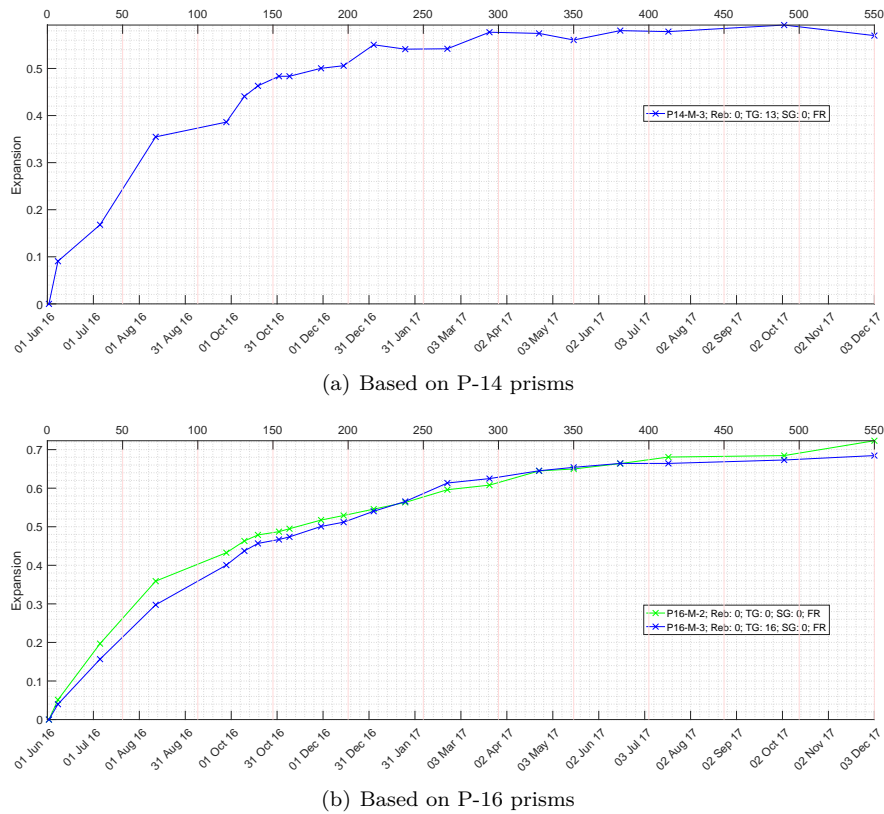


Figure 6.2: AAR expansion in tested concrete specimens

6.4 Test Results

Table 6.1 is now extended to include additional data and is sorted by group numbers (A-H), Table 6.2, and includes:

1. Test ID.
2. Batch (there were a total of 4).
3. Presence or not of reinforcement. Presence of reinforcement implies testing a structural element, absence corresponds to material testing (to the extent possible).
4. 28 days compressive strength. Unfortunately, no tests could be performed at the age of the specimen testing (not enough specimens could be cast).
5. One year splitting tensile strength.
6. Confining forces.
7. Peak recorded shear force during the test.
8. Peak force normalized with respect to the square root of the 28 days compressive strength ((ACI 318-14, 2014) specifies that the shear strength is a function of the square root of the compressive strength).
9. Peak force normalized with respect to the 28 days compressive strength.
10. Peak force normalized with respect to the one year splitting tensile strength.

When more than one data point is available, mean and normalized standard deviations are also listed.

Table 6.2: Experimental results

| ID | Batch | Reinf. | f_c | f_t | Conf. | $P1$ | $P2$ | $P3$ | $P4$ |
|---|-------|--------|---------|--------|----------|----------------|------------------|-----------|----------|
| | | | 28 days | 1 year | Force | Exp. P_{max} | $P1/\sqrt{f'_c}$ | $P1/f'_c$ | $P1/f_t$ |
| | | | ksi | | Kips | | - | - | - |
| A: AAR, Reinforcement, Normal confinement | | | | | | | | | |
| 1 | 1 | Y | 6 | 0.43 | 88.0 | 235 | 96 | 39 | 546 |
| 2 | | | | | | 209 | 85 | 35 | 485 |
| 3 | | | | | | 238 | 97 | 40 | 554 |
| 5 | 2 | Y | 5 | 0.4 | 88.0 | 214 | 96 | 43 | 536 |
| 6 | | | | | | 221 | 99 | 44 | 553 |
| 7 | | | | | | 232 | 104 | 46 | 581 |
| 9 | 3 | Y | 4.2 | 0.3 | 88.0 | 220 | 107 | 52 | 732 |
| | | | | | Mean | 224 | 98 | 43 | 569 |
| | | | | | std/Mean | 5.0% | 7.2% | 13.3% | 13.6% |
| B: AAR, Reinforcement, Low confinement | | | | | | | | | |
| 10 | 3 | Y | 4.2 | 0.3 | 44.0 | 182 | 89 | 43 | 606 |
| C: AAR, Reinforcement, High Confinement | | | | | | | | | |
| 11 | 3 | Y | 4.2 | 0.3 | 100.0 | 243 | 119 | 58 | 810 |
| D: AAR, No Reinforcement, Normal Confinement | | | | | | | | | |
| 4 | 2 | N | 5 | 0.4 | 88.0 | 156 | 70 | 31 | 390 |
| 8 | | | | | | 160 | 71 | 32 | 399 |
| 12 | 3 | Y | 4.2 | 0.3 | 88.0 | 162 | 73 | 32 | 406 |
| | | | | | Mean | 159 | 71.3 | 31.9 | 398.4 |
| | | | | | std/Mean | 2.0% | 2.0% | 2.0% | 2.0% |
| E: AAR, No Reinforcement, High confinement | | | | | | | | | |
| 12 | 3 | N | 4.2 | 0.3 | 100.0 | 162 | 79 | 39 | 541 |
| F: NO AAR, Reinforcement, Normal Confinement | | | | | | | | | |
| 13 | 4 | Y | 5.7 | 0.68 | 88.0 | 286 | 120 | 50 | 421 |
| 14 | | | | | | 284 | 119 | 50 | 418 |
| | | | | | Mean | 285 | 119.50 | 50.05 | 419.56 |
| | | | | | std/Mean | 0.58% | 0.58% | 0.58% | 0.58% |
| G: NO AAR, NO Reinforcement, Normal Confinement | | | | | | | | | |
| 16 | 4 | N | 5.7 | 0.68 | 88.0 | 195 | 82 | 34 | 287 |
| H: NO AAR, No Reinforcment, High Confiement | | | | | | | | | |
| 15 | 4 | N | 5.7 | 0.68 | 100.0 | 225 | 94 | 39 | 330 |

Concrete strengths are tabulated in Tables 3.1 and 3.2.

6.5 Finite Element Simulation

Finite element simulation of the tests was performed with our computer code Merlin (Saouma, Červenka, and Reich, 2010) and (Saouma, 2003). The same code was used in the computational aspect of this project (Saouma, 2017). A final AAR expansion of 0.5% was assumed based on Fig. 6.2.

Results of the finite element simulations are shown in Table 6.3 along with the corresponding experimental peak shear forces. This table calls for the following clarifications:

- The finite element analysis has to begin with the 28 days compressive and tensile strengths.
- In the absence of splitting tensile strength measurements at 28 days, it is assumed that $f_t = 9\sqrt{f'_c}$.
- It is assumed that f'_c and f_t remain constant throughout the one year before the non-reactive specimens are tested. The reactive specimens are assumed to degrade by a factor β .
- β is computed as the ratio of the one year measured tensile strength over the estimated 28 days one ($\beta = f_t/f_{t0} = f_t/\sqrt{f'_c}$)
- The initial elastic modulus is estimated as $E_{ini} = 57,000\sqrt{f'_c}$.
- It is assumed that the elastic modulus decreases throughout the AAR in the same proportion as the tensile strength, hence $E_{final} = \beta E_{ini}$.

Based on the preceding assumptions, 7 analyses were performed (corresponding to A, B, C, D, F, G and H groups). Results are tabulated in Table 6.3.

Table 6.3: Details and results of FEA along with experimental results

| Test | desc. | Reinf | Material properties and tractions | | | | | | | Peak Load | | |
|--------|--------|-------|-----------------------------------|----------|-------|---------|-----------|-------------|----------|-----------|-------|--------|
| | | | f'_c | f_{t0} | f_t | β | E_{ini} | E_{final} | Traction | Exp. | Num. | % Diff |
| Series | | | psi | psi | psi | | e+06 psi | | psi | kips | kips | |
| A | AAR | Y | 5,000 | 636 | 400 | 0.63 | 4.03 | 2.53 | 333 | 219.7 | 242.8 | 9.4% |
| B | AAR | Y | 4,200 | 583 | 300 | 0.51 | 3.69 | 1.90 | 147 | 182.0 | 175.3 | -3.7% |
| C | AAR | Y | 4,200 | 583 | 300 | 0.51 | 3.69 | 1.90 | 333 | 243.0 | 213.6 | -12.1% |
| D | AAR | N | 5,000 | 636 | 400 | 0.63 | 4.03 | 2.53 | 333 | 159.0 | 134.9 | -14.4% |
| E | AAR | N | 4,200 | 583 | 300 | 0.51 | 3.69 | 1.90 | 333 | 162.0 | - | - |
| F | NO AAR | Y | 5,700 | 680 | 680 | 1.00 | 4.30 | 4.30 | 293 | 285.0 | 303.5 | 6.5% |
| G | NO AAR | N | 5,700 | 680 | 680 | 1.00 | 4.30 | 4.30 | 293 | 195.0 | 168.6 | -13.5% |
| H | NO AAR | N | 5,700 | 680 | 680 | 1.00 | 4.30 | 4.30 | 333 | 225.0 | 191.1 | -14.7% |

The numerically computed load displacement curves are shown in Fig. 6.3(a) and 6.3(b). The corre-

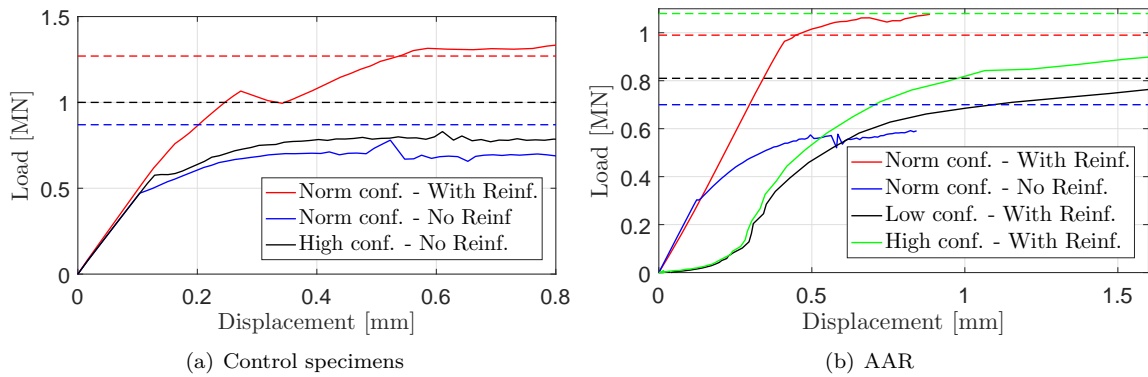


Figure 6.3: FEA computed load displacement curves.

sponding experimental results are shown simply as an asymptotic horizontal peak value as experimentally the measured actuator stroke included substantial elastic deformation of the blue cage inside which the

specimen was placed, Fig. 1.3.

Finally, Fig. 6.4 shows the extent of internal cracking corresponding to various points in the load displacement curve.

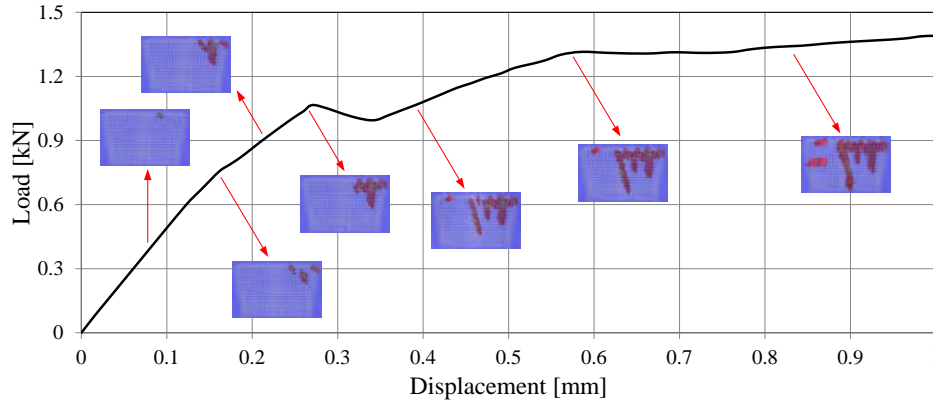


Figure 6.4: Computed internal cracking in terms of load displacement curve

6.6 Analysis of Results

Fig. 6.5 summarizes all experimental and numerical results in a single diagram. As absolute values, these results are of relatively minor importance, and one must normalize them (as dictated by the questions raised in Sect. 6.2), Fig. 6.6, to draw proper conclusions.

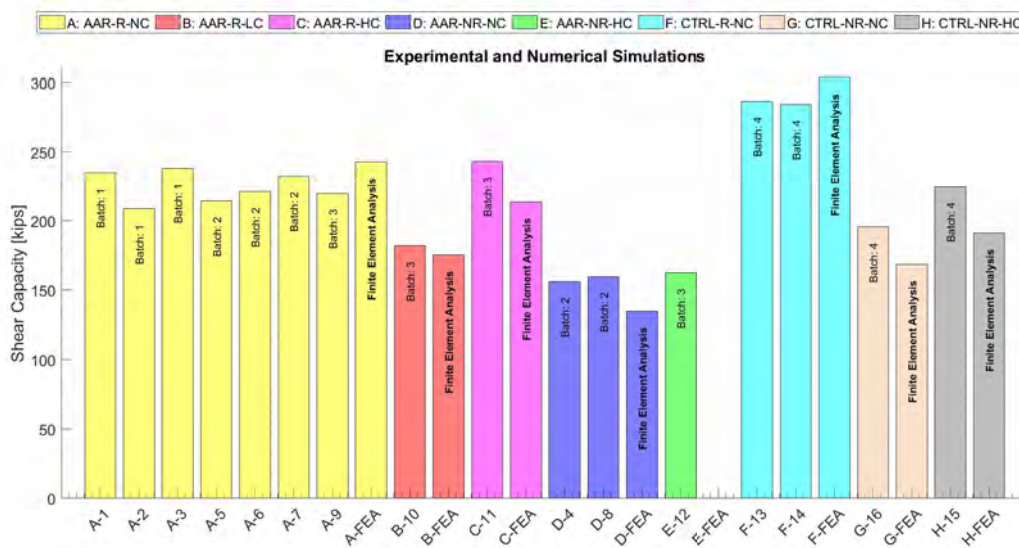


Figure 6.5: Experimental and numerical results

1. Test results are remarkably close within a given group. The normalized standard deviations for series A, D, and F (where more than one test is available) are 5.0, 2.0, and 0.58 percent respectively, Table

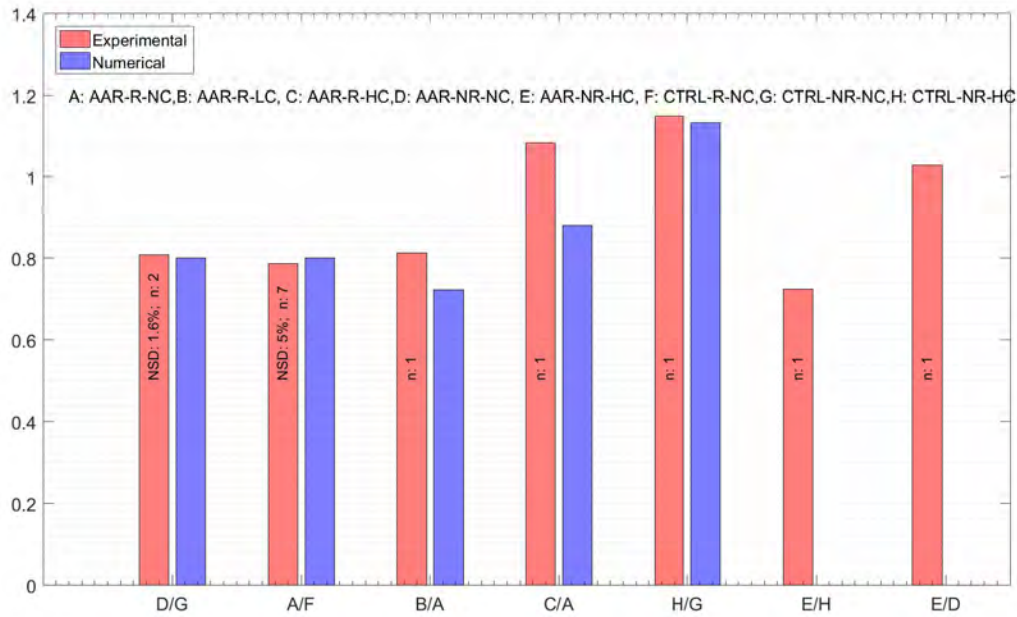


Figure 6.6: Normalized experimental and numerical results

6.2 and Fig. 6.5. This reinforces the reliability of the test program.

2. Tested specimens underwent an approximate AAR expansion of 0.5% Fig. 6.2.
3. The finite element simulations captured well the experimental results, Fig. 6.6.
4. The AAR causes a $\approx 20\%$ reduction in shear strength for reinforced concrete specimens (structural effect) under base confinement; A/F in Fig. 6.6.
5. The AAR causes a $\approx 20\%$ reduction in shear strength for unreinforced concrete specimens (material effect) under base confinement; D/G in Fig. 6.6.
6. The AAR causes a $\approx 20\%$ reduction in shear strength for unreinforced concrete specimens (material effect) under high confinement; E/H in Fig. 6.6.
7. A reduction in confinement (from 88 to 44 in Table 6.2 for reinforced concrete panels with AAR resulted in a reduction in shear strength of $\approx 20\%$; B/A in Fig. 6.6.
8. An increase in confinement (from 88 to 100 in Table 6.2 for reinforced concrete panels with AAR resulted in an increase in shear strength of $\approx 10\%$; C/A in Fig. 6.6. This effect is not well captured numerically.
9. An increase in confinement (from 88 to 100 in Table 6.2 for unreinforced concrete panels with AAR resulted in an increase in shear strength of $\approx 10\%$; E/D in Fig. 6.6.
10. An increase in confinement (from 88 to 100 in Table 6.2 for unreinforced concrete panels without AAR resulted in an increase in shear strength of $\approx 20\%$; H/G in Fig. 6.6.
11. When experimental shear strength $P1$ are normalized with respect to $\sqrt{f'_c}$, f'_c and f_t ($P2$, $P3$, and $P4$ respectively) for all test series, Table 6.4, the lowest normalized standard deviations are associated with $P1$ and $P2$. Non reactive concrete exhibit slightly higher values (18% vs 16%), however this may be due to limited number of data points (4 instead of 12).
12. Shear strength degradation $\approx 20\%$ is lower than the splitting tensile strength decrease ($\approx 50\%$), Fig.

3.19.

All those results were anticipated, but were not quantifiable until this present research program.

Table 6.4: Statistical analysis of results

| | <i>P1</i> | <i>P2</i> | <i>P3</i> | <i>P4</i> |
|---------------------------------|----------------------------------|------------------|-----------|-----------|
| | Exp. P_{max} | $P1/\sqrt{f'_c}$ | $P1/f'_c$ | $P1/f_t$ |
| A, B, C, D, E Cumulative | | | | |
| Mean | 202.64 | 91.11 | 41.15 | 549.20 |
| std/Mean | 16% | 16% | 19% | 22% |
| F, G, H Cumulative | | | | |
| Mean | 247.65 | 103.73 | 43.45 | 364.19 |
| std/Mean | 18% | 18% | 18% | 18% |

This page intentionally left blank.

7— Observations and Conclusions

To the best of our knowledge, this was the most comprehensive study on the effect of AAR on the shear strength of concrete.

16 large specimens were carefully prepared, and tested through a unique test apparatus designed for shear testing.

Varied was the presence/absence of reinforcement, confining traction, and results compared with a set of control specimens.

Finite element simulations succeeded in capturing the response, and the code (Merlin) was thus validated in properly modeling AAR with a structure subjected to AAR.

In summary, it may be safely stated that AAR will reduce the shear strength by $\approx 20\%$.

This page intentionally left blank.

Bibliography

- ACI 318-14 (2014). *Building code requirements for structural concrete (ACI 318-14) and commentary*. Tech. rep. American Concrete Institute.
- ADAMS Accession No. ML 121160422 (2012). *Impact of Alkali Silica Reaction on Seabrook Concrete Structure*. Tech. rep. NextEra.
- Amberg, F. (2011). “Performance of dams affected by expanding concrete”. In: *Dams and Reservoirs under Changing Challenges*, p. 115.
- ASTM, C39 (2016). “39, Standard test method for compressive strength of cylindrical concrete specimens”. In: *Annual book of ASTM standards* 04.02.
- ICOLD Bulletin 79 (1991). *Alkali-Aggregate Reaction in Concrete Dams*. Tech. rep. International Commission on Large Dams.
- Murazumi, Y. et al. (2005a). “Study of the influence of alkali-silica reaction on mechanical properties of reinforced concrete members”. In: *18th International Conference on Structural Mechanics in Reactor Technology (SMIRT 18)*. SMIRT18-H03-3. Beijing, China, pp. 2043–2048.
- Murazumi, Y. et al. (2005b). “Study of the influence of Alkali-Silica Reaction on structural behavior of reinforced concrete members”. In: *18th International Conference on Structural Mechanics in Reactor Technology (SMIRT 18)*. SMIRT18-H03-2. Beijing, China, pp. 2036–2042.
- Naus, D. (2007). *Primer on Durability of Nuclear Power Plant Reinforced Concrete Structures - A Review of Pertinent Factors*. Tech. rep. NUREG/CR-6927 ORNL/TM-2006/529. U.S. Nuclear Regulatory Commission.
- NUREG/CR-6706 (2001). *NUREG/CR-6706: Capacity of Steel and Concrete Containment Vessels With Corrosion Damage*. URL: <http://pbadupws.nrc.gov/docs/ML0110/ML011070123.pdf>.
- Orbovic, N. (2011). *Personal Communication*. Canadian Nuclear Safety Commission.
- Orbovic, N. et al. (2015). “Alkali Aggregate Reaction in Nuclear Concrete Structures: Part 1: A Holistic Approach”. In: *Proceedings of the 23rd Conference on Structural Mechanics in Reactor Technology (SMiRT23)*.
- Saouma, V. (2003). *Theory Manual for the Merlin Finite Element Program*. Tech. rep. Tokyo Electric Power Service Company (TEPSCO), Tokyo. URL: <http://civil.colorado.edu/~saouma/Merlin>.
- (2013). “Applications of the cohesive crack model to concrete, ceramics and polymers”. In: *Proceedings of the 8th International Conference on the Fracture Mechanics of Concrete and Structures*. Invited Pleanry Lecture. Toledo, Spain.
- Saouma, V.E. (2017). *Probabilistic Based Nonlinear Seismic Analysis of Nuclear Containment Vessel Structures with AAR*. Tech. rep. Final Report to NRC, Grant No. NRC-HQ-60-14-G-0010, Task 3-B. University of Colorado, Boulder.

- Saouma, V.E., R. Sparks, and D. Graff (2016). *Development Of ASR Concrete Mix for Large Scale Testing*. Tech. rep. Report to the Nuclear Regulatory Commission, Grant No. NRC-HQ-60-14-G-0010. University of Colorado, Boulder.
- Saouma, V.E., J. Červenka, and R. Reich (2010). *Merlin Finite Element User's Manual*. URL: <http://civil.colorado.edu/~saouma/pdf/users.pdf>.
- Saouma, V.E. et al. (2016). *AAR Expansion; Effect of Reinforcement, Specimen Type, and Temperature*. Tech. rep. Report to the Nuclear Regulatory Commission, Grant No. NRC-HQ-60-14-G-0010. University of Colorado, Boulder.
- Shimizu, H. et al. (2005a). "Investigaiton of Safety Margin for Turbine Generator Foundation Affected by Alkali-Silica Reaction Based on Non-Linear Structural Analysis". In: *18th International Conference on Structural Mechanics in Reactor Technology (SMIRT 18)*. SMIRT18-H03-4. Beijing, China, pp. 2049–2059.
- Shimizu, H. et al. (2005b). "Study on Material Properties in Order to Apply for Structural Analysis of Turbine Generator Foundation Affected by Alkali-Silica Reaction". In: *18th International Conference on Structural Mechanics in Reactor Technology (SMIRT 18)*. SMIRT18-H03-5. Beijing, China, pp. 2055–2060.
- Takagkura, T. et al. (2005). "Structural soundness for turbine-generator foundation affected by alkali-silica reaction and its maintenance plans". In: *18th International Conference on Structural Mechanics in Reactor Technology (SMIRT 18)*. SMIRT18-H03-5. Beijing, China, pp. 2055–2060.
- Takatura, T. et al. (2005a). "Investigation of the expanded value of turbine generator foundation affected by alkali-silica reaction". In: *18th International Conference on Structural Mechanics in Reactor Technology (SMIRT 18)*. SMIRT18-H03-7. Beijing, China, pp. 2061–2068.
- Takatura, T. et al. (2005b). "Vibration measurement and simulation analysis on a reinforced concrete structure with alkali-silica reaction". In: *18th International Conference on Structural Mechanics in Reactor Technology (SMIRT 18)*. SMIRT18-H03-1. Beijing, China, pp. 2026–2035.
- Tcherner, J. and T. Aziz (2009). "Effects of AAR on Seismic Assessment of Nuclear Power Plants for Life Extensions". In: *20th International Conference on Structural Mechanics in Reactor Technology (SMIRT 20)*. SMIRT20-Division 7 Paper 1789. Espoo, Finland.

Index

- Anchorage, [19](#)
- Assembly of Test Setup, [87](#)
- Burlap, [26](#), [31](#), [32](#)
- Casting, [26](#)
- Cheklis, [39](#)
- Compressive Strength, [29](#)
- Conceptual Model, [14](#)
- Conclusions, [75](#)
- Concrete
 - Compressive Strength, [50](#)
 - Splitting Tensile Strength, [50](#)
- Control, [82](#)
- Curing, [30](#)
- Data Acquisition and Control, [79](#)
- Data safeguard, [57](#)
- Demec, [33](#)
- Dimensions, [14](#)
- Eaton Hydraulics Actuators, [82](#)
- Eaton Vickers Valves, [82](#)
- End Plates, [17](#)
- Expansion Measurements, [33](#), [67](#)
- Fall Line Inspections LLC, [25](#)
- Finite Element Simulation, [69](#)
- Fog Room, [30](#)
- Forklift, [31](#)
- Formwork, [25](#)
- Hydraulics, [83](#)
- Installation Procedure, [38](#)
- Instrumentation, [80](#)
- LabVIEW, [56](#), [79](#)
- LabView Operation, [56](#)
- Leaching, [31](#)
- Load Determination, [21](#)
- Load Transfer Mechanism, [14](#)
- Million Pound Test Frame, [14](#)
- Model, [14](#)
- Motivation, [13](#)
- MTS Calibration, [85](#)
- National Instruments, [79](#)
- National Instruments PXI, [53](#)
- NCVS to Specimen, [20](#)
- Notch, [37](#)
- Pans, [31](#)
- Pictures
 - Post-Mortem, [61](#)
 - Pre-Tests, [42](#)
- Post-Mortem, [59](#)
- Prototype, [14](#)
- Questions to be Addressed, [67](#)
- Reinforcement, [17](#)
- Servovalve, [54](#)
- Shear Reinforcement, [13](#)
- Shearing Force, [81](#)
- Shrinkage, [26](#)
- Sodium Hydroxide, [32](#)
- Specimen Removal, [37](#)
- Splitting Tensile Strength, [37](#)
- Sprinkler Systems, [32](#)
- Strain Gage, [26](#)
- Structures Lab, [30](#)
- Temperature Gage, [26](#)

Test Configurations, [66](#)

Test Matrix, [66](#)

Test Notes, [59](#)

Test Preparation, [53](#)

Test Results, [68](#)

Test Setup, [14](#)

Test Termination, [57](#)

Testing Protocol, [37](#)

Wiring connections, [53](#)

A— Test Data Acquisition and Control

An essential part of the experiment is a system to control the loading via the three actuators and to measure the results using various sensors. These various components have not been used together in some time, and the original electronic systems used for control and measurement are either not functional or not up to the task of this experiment. As such a new system is being developed using mostly existing hardware present in the laboratory.

The loading forces are applied using three hydraulic actuators. One will provide the shear loading and the other two will provide containing loads. The shear loading actuator is part of a compression load frame made by Material Test Systems (MTS) and has its own controller which will also measure the shear force and displacement, Fig. A.1. The two containing actuators, Fig. A.2, manufactured by Eaton with a 160-kip capacity, do not have their own controller and so one is being developed. This controller will use oil pressures to determine the containing force, and operate variable valves accordingly to maintain desired forces.



Figure A.1: MTS million-pound load frame

The core of the control and measurement will be happening in a National Instruments (NI) system and programmed in the LabVIEW programming language, Fig. A.3. This system is responsible for the overall



Figure A.2: Eaton hydraulic actuators

motion and forces of the experiment, as well as aggregating all measurements for recording. It will directly control the containing actuator valves and send a signal to the MTS controller to control the shear actuator. The NI system will take measurements from the MTS controller as well as measurements from its own sensors including oil pressure, crack mouth opening displacement, and crack sliding displacement.



Figure A.3: National Instruments PXI-1042Q with embedded controller, data acquisition, and command

A.1 Instrumentation

The goal of the experiment is to take measurements that will provide adequate data for the failure analysis of the specimens. The data will help us understand when and how the shear cracks develop. To reach this goal, a number of sensors will measure the forces applied to the specimens and how different areas of the specimens move relative to each other.

All sensors ultimately terminate in the National Instruments' PXI-1042 with embedded controller system (the NI DAQ). This system has been selected because it is more modern than most of the existing control equipment and is very versatile. It can be easily adapted to meet the needs of this experiment as well as be reprogrammed if the needs of the experiment change. In addition, it is reliable and the conditioning modules provide stable signals from the sensors. A LabVIEW program makes timed measurements of all sensor channels and records the data to a file. In turn, the sensor readings are available to the control portion of the LabVIEW program.

The containing force needs to be measured so that the sample can be placed under a constant load and that the load can be verified as matching the analytical calculations. It is determined by measuring the pressure of the oil pushing on the hydraulic pistons, and the pressure of the oil pushing against the hydraulic pistons. The two Omega Engineering pressure transducers, Fig. A.4 connect to the SCXI-1520 conditioning module in the NI DAQ. A calibration with a MTS load cell is performed to correlate the pressure readings with forces.



Figure A.4: Omega pressure transducer

The shearing force also needs to be measured to understand how much energy was needed to open the shear crack. It is measured by a MTS load cell mounted on the crosshead of the MTS million-pound load frame. This load cell connects to the MTS control system. The shear cage's displacement is measured by a LVDT, Fig. A.5, mounted on the actuator of the MTS million-pound load frame and also connected to the MTS control system. Both sensors are conditioned by the MTS control system and are output as DC voltages that connect to the SCXI-1520 module in the NI DAQ.

The original goal of having crack mouth opening and crack sliding displacement sensors and to control by those sensors wasn't implemented due to time and cost constraints. However a single LVDT to measure the crack opening was added to the system. This half-inch-stroke LVDT was positioned such that it spanned the region most likely to develop the main shear crack, and placed at an angle perpendicular to the crack's direction so that its main measurement would be the crack opening. It was connected to the DAQ system via a SCXI-1540 module with SCXI-1315 terminal block that conditioned the AC LVDT signals. The LVDT was a Sentech 75PCAC-250.

Another addition was the measurement of strain in the blue cage. The goal was to better model how load was being transferred from the vertical shearing forces through the blue cage to the specimen. Two rosette-style gauges were added on the triangular side pieces to measure strain in two directions, and two single-element strain gauges were added on the narrow end pieces near the corners to measure vertical strain in those pieces. The strain gauges were model Omega KFH-3-120-D17-11L1M2S and were connected into a SCXI-1520 strain module with SCXI-1314 terminal block that conditioned the strain signals and provided



Figure A.5: LVDT body

the completion bridges.

A.2 Control

To achieve good measurements, care is taken to develop the system such that it provides calculated and accurate movements and forces. These forces are large but must be handled in a controlled fashion so as to be able to take as many measurements as possible. Quick or unexpected forces could damage the specimen before useful data is collected and so all of the forces are controlled by a computer built specifically for the control and measurement of physical systems. Software is being written to handle the specific requirements of this experiment.

Control of the containing force is achieved by the LabVIEW program using readings from the pressure transducers. The operator enters a desired containing force and the LabVIEW program compares that force to the measured force. The program computes a signal which opens Eaton Vickers valves to move the attached Eaton Hydraulics actuators. The commanded force remains static during the test and an integrating-proportional control loop is used to signal the valves to increase or decrease the oil pressure in the Eaton actuators. This changes the load applied through the horizontal tension rods to both sides of the sample.

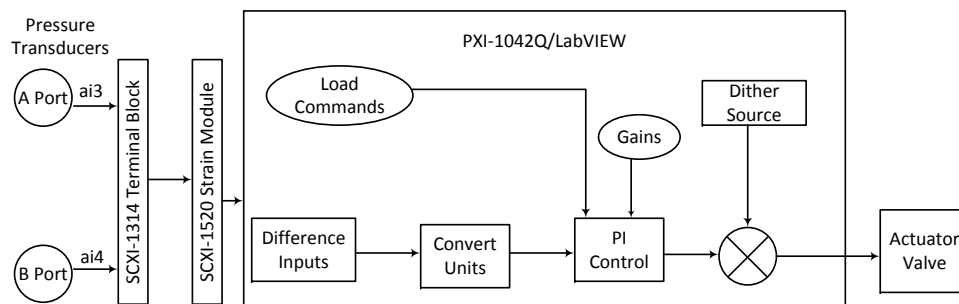


Figure A.6: Pressure-control flow diagram

Control of the shearing motion is achieved by the LabVIEW program and the MTS control system using readings from the shearing actuator's LVDT Fig. A.7. The commanded opening is a constant rate by outputting an offset displacement voltage to the MTS control system.

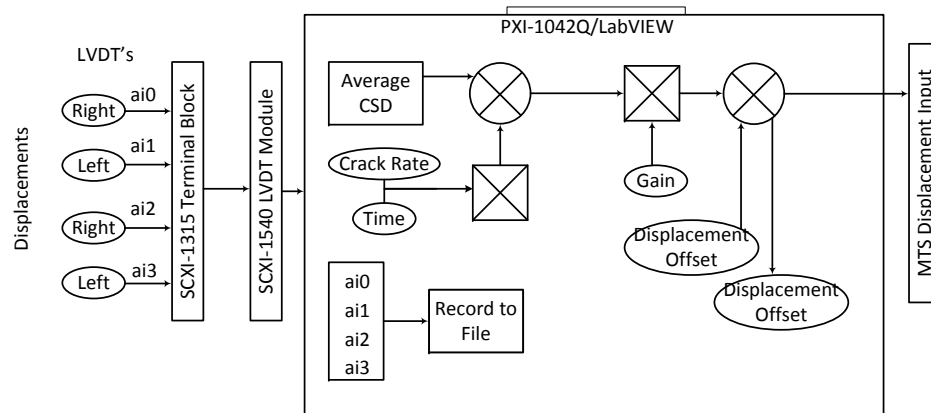


Figure A.7: Crack opening flow diagram

A.3 Hydraulics

Achieving large forces in a controlled fashion requires the use of hydraulic actuators. These actuators use hydraulic pressure to move their pistons which are connected to various parts of the specimens. The hydraulic pressure is regulated by precision valves which receive electrical signals from the controlling computer.

During this test there are two hydraulic servo valves regulating the hydraulic oil. One will regulate the MTS shear actuator. This valve is controlled by the MTS control system, with further input from the NI DAQ.

The other will regulate the two containing actuators, with the oil for both actuators flowing through the same valve. The actuators will apply the same force because they share the same pressure. This valve is controlled directly by the NI DAQ, using a DC voltage signal.

Intermediate oil pressure is provided by the hydraulic service manifold (HSM). The HSM only has three operating modes: off, low, and high. The HSM therefore doesn't control the fine movements of the actuators but rather serves as a safety shutoff and allows for reduced pressure during development.

Oil pressure for all three actuators is provided by two MTS 70-gallon-per-minute pumps. They are a variable displacement type with associated plumbing and hardware to control the oil flow and cooling. The output from the pumps is a constant 3,000 PSI.

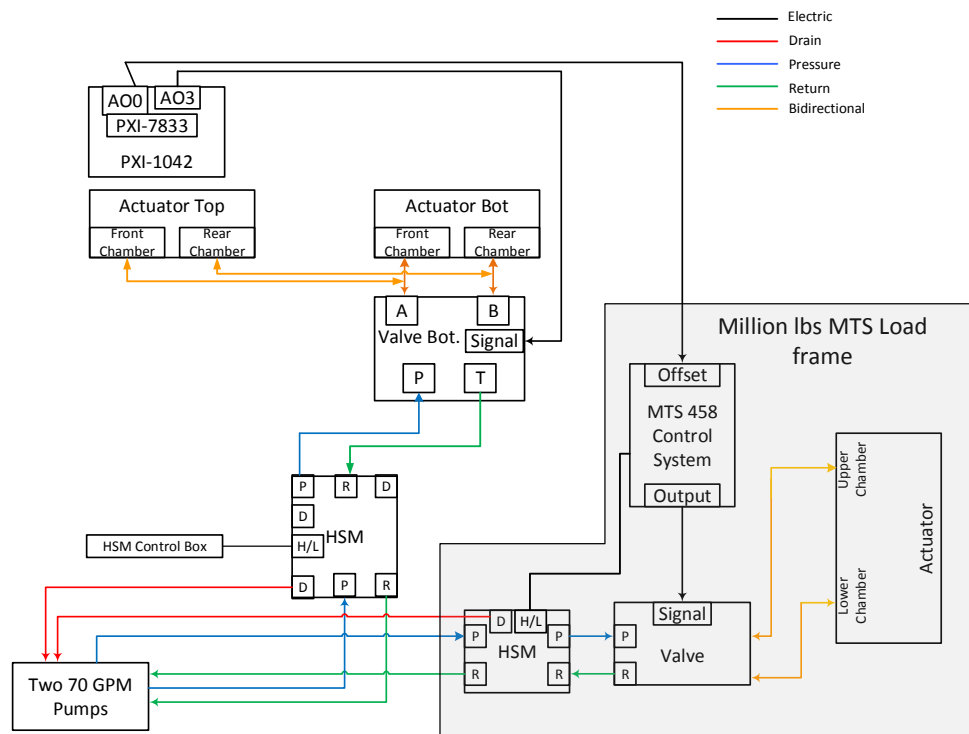


Figure A.8: Hydraulic oil distribution and command

B— Calibration

B.1 MTS Calibration

To ensure proper and reliable load/displacement measurements, the testing machine was calibrated by MTS, and official calibration sheets were provided, Fig. B.1.



Figure B.1: Calibration of the Million lbf MTS

This page intentionally left blank.

C— Assembly of Test Setup

Assembly of the test setup started. Regretfully, tolerances had not been specified, which implies that though all the parts fit together, this required much effort to “hammer in” various components, Fig. C.1.

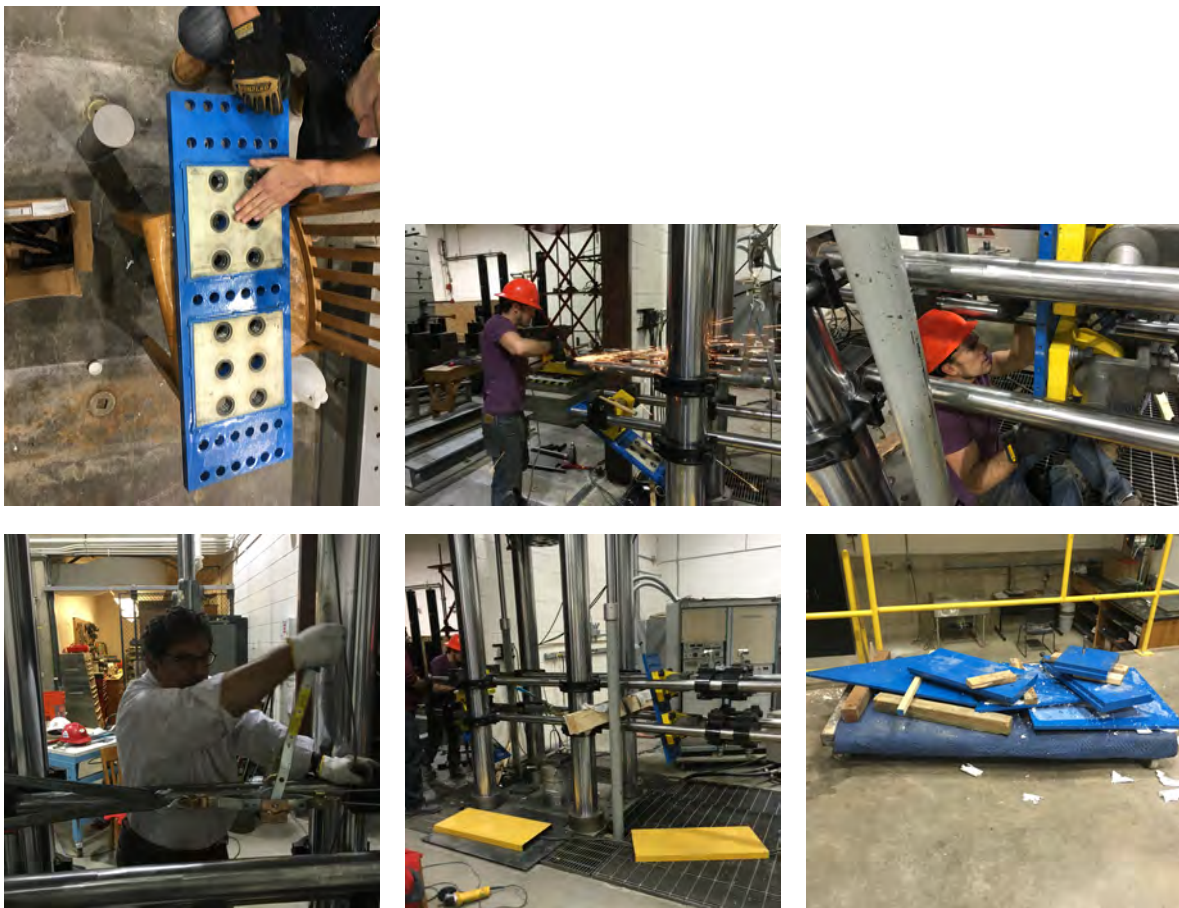


Figure C.1: Setup Installation as of Jan 15. Specimen “cage” (lower right) will be assembled and proof tested next

Finally, the assembly process is shown in Fig. C.2.



(a) Cleaned and powder-coated components



(b) Sample frame components undergoing initial assembly



(c) Sample end plates with welded shear studs



(d) Reaction bars awaiting assembly

Figure C.2: Assembly of test setup